

ELECTROCHEMICAL COPOLYMERIZATION OF EDOT AND N-PHENYLSULFONYL PYRROLE: MORPHOLOGIC, SPECTROSCOPIC, ELECTROCHEMICAL CHARACTERIZATIONS

**M.Sc. Thesis by
Cansev TEZCAN**

Department : Polymer Science and Technology

Programme : Polymer Science and Technology

JUNE 2010

**ELECTROCHEMICAL COPOLYMERIZATION OF EDOT AND N-
PHENYLSULFONYL PYRROLE: MORPHOLOGIC, SPECTROSCOPIC,
ELECTROCHEMICAL CHARACTERIZATIONS**

**M.Sc. Thesis by
Cansev TEZCAN
(515081004)**

**Date of submission : 07 May 2010
Date of defence examination: 09 June 2010**

**Supervisor (Chairman) : Prof. Dr. A.Sezai SARAÇ (ITU)
Members of the Examining Committee : Assis. Prof. Dr. Orhan GÜNEY (ITU)
Assis. Prof. Dr. Ramazan KIZIL (ITU)**

JUNE 2010

İSTANBUL TEKNİK ÜNİVERSİTESİ ★ FEN BİLİMLERİ ENSTİTÜSÜ

**EDOT VE N-FENİLSÜLFONİL PİROLÜN ELEKTROKİMYASAL
KOPOLİMERİZASYONU: MORFOLOJİK, SPEKTROSKOPİK,
ELEKTROKİMYASAL KARAKTERİZASYONLARI**

**YÜKSEK LİSANS TEZİ
Cansev TEZCAN
(515081004)**

Tezin Enstitüye Verildiği Tarih : 07 Mayıs 2010

Tezin Savunulduğu Tarih : 06 Haziran 2010

**Tez Danışmanı : Prof. Dr. A.Sezai SARAÇ (İTÜ)
Diğer Jüri Üyeleri : Doç. Dr. Orhan GÜNEY (İTÜ)
Yrd. Doç. Dr. Ramazan KIZIL (İTÜ)**

HAZİRAN 2010

FOREWORD

Firstly, I would like to thank my advisor, Prof.Dr. A.Sezai SARAÇ, for his encouragement, incomparable advices, guidance and discussions in my studies and I have had to learn across broad disciplines, to develop as a scientist.

I would like to offer the most grateful and special thanks to Prof.Dr. Gözen BEREKET for her support and help.

I thank to my old friend *Ebru ATABEYOGLU* for her valuable friendship for 14 years.

I would like to thank to my family, especially my father Remzi TEZCAN and my sister Dr. Nurcan TEZCAN ERGIN for precious critics against some of my opinions, respect to my decisions and being always with me at every stage of my life.

My personal thanks goes to Semih UZUN for his full support, patience, understanding and being always with me during these two years.

I wish to express my special thanks to all Electropol-Nanotech Group members for all their help. Damla ECEVIT, Timucin BALKAN, Asli GENCTURK, N.Ugur KAYA, Suat CETINER, Fatma GULER and Ulviye DALGIC, with all of you, it has really been a great pleasure.

Also I would like to thank my old friend Nilgun KILIC for her full support.

And finally, all my praises to God, from whom all blessings below.

June 2010

Cansev TEZCAN

TABLE OF CONTENTS

	<u>Page</u>
FOREWORD.....	v
TABLE OF CONTENTS.....	vii
ABBREVIATIONS	ix
LIST OF TABLES	xi
LIST OF FIGURES	xiii
SUMMARY	xv
ÖZET.....	xvii
1. INTRODUCTION.....	1
1.1 Conductive Polymers	1
1.1.1 Use of conducting polymers	3
1.1.2 Band gap theory	6
1.1.3 Doping and electrical conductivity	8
1.1.4 Optical properties	10
1.2 Electrochemical Polymerization	10
1.2.1 Chronoamperometry	11
1.2.2 Chronopotentiometry	12
1.2.3 Factors affected the electropolymerization	12
1.2.3.1 Monomer substitution.....	12
1.2.3.2 Effect of the electrolyte	13
1.2.3.3 Effect of the cation	13
1.2.3.4 Effect of the solvent	14
1.2.3.5 Effect of the temperature.....	15
1.2.3.6 Scan rate dependencies	15
1.2.4 PXDOT derivatives	16
1.2.5 PEDOT.....	17
1.2.6 N-Phenylsulfonyl pyrrole.....	18
1.3 Carbon Fiber Microelectrodes.....	19
1.4 Electrochemical Impedance Spectroscopy (EIS)	21
1.4.1 Equivalent circuit elements	26
1.4.1.1 Electrolyte resistance	29
1.4.1.2 Double layer capacitance	29
1.4.1.3 Polarization resistance.....	29
1.4.1.4 Diffusion	30
1.4.1.5 Constant phase element.....	30
1.5 Characterizations	31
1.5.1 FTIR-ATR.....	31
1.5.2 Spectroelectrochemistry	31
1.5.3 Scanning electron microscopy (SEM)	32
1.5.4 Atomic force microscopy (AFM)	33
2. EXPERIMENTAL	37
2.1 Chemicals	37

2.2 Electrocopolymerization.....	37
2.3 Electrode Preparations.....	37
2.4 Electrochemical Impedance Spectroscopy and Equivalent Circuit Modelling	38
2.5 FTIR-ATR	39
2.6 Ultra-Violet/Visible Spectrophotometric Measurements	39
2.7 Scanning Electron Microscope.....	39
2.8 Atomic Force Microscopy	39
3. RESULTS AND DISCUSSIONS	41
3.1 The Experimental Details	41
3.2 Electrocopolymerization of EDOT and PSP	42
3.3 Ex-situ FTIR-ATR Measurements of Poly(EDOT-co-PSP) and PEDOT	45
3.4 Ex-situ UV-Vis Spectrophotometric Msrmts of EDOT-PSP Oligomers	49
3.5 EIS Investigation and ECM of Poly(EDOT-co-PSP).....	50
3.6 Morphological Analyses of Poly(EDOT-co-PSP) via SEM and AFM	57
4. CONCLUSION.....	61
REFERENCES.....	63
CURRICULUM VITAE	72

ABBREVIATIONS

AC	: Alternating Current
ACN	: Acetonitrile
AFM	: Atomic Force Microscopy
CA	: Chronoamperometry
CF	: Carbon Fiber
CP	: Conducting Polymer
CPE	: Constant Phase Element
CV	: Cyclic Voltammetry
C_{DL}	: Double Layer Capacitance
C_{LF}	: Low Frequency Capacitance
DC	: Direct Current
DMF	: Dimethylformamide
DMSO	: Dimethylsulfoxide
ECD	: Electrochromic Devices
ECM	: Equivalent Circuit Modelling
EDOT	: 3,4-Ethylenedioxythiophene
EPR	: Electro Paramagnetic Resonance
ESR	: Electro Spin Resonance
FTIR-ATR	: Foruier Transform Infrared-Attenuated Total Reflection
HOMO	: High Occupied Molecular Orbital
MMA	: Methylmetacrylate
MO	: Molecular Orbital
NaClO₄	: Sodium Perchlorate
PAN	: Polyacrylonitrile
PC	: Propylenecarbonate
PEDOT	: Poly(3,4-Ethylenedioxythiophene)
PPy	: Polypyrrole
PSP	: Phenylsulfonyl pyrrole
PTh	: Polythiophene
R	: Alkyl group
SCFME	: Single Carbon Fiber Micro Electrode
SEM	: Scanning Electron Microscope
UV-Vis	: Ultraviolet-Visible

LIST OF TABLES

	<u>Page</u>
Table 1.1: Common electrical elements	26
Table 1.2: Circuit elements used in the models.	27
Table 3.1: FTIR-ATR assignments of Poly(EDOT-co-PSP)s	47
Table 3.2: ΔQ , thickness of copolymr coated SCFME, C_{LF} and phase angle values for different molar ratios of Poly(EDOT-co-PSP)	52
Table 3.3: Mole fraction dependence of parameters calculated from the equivalent circuit model for PEDOT and Poly(EDOT-co-PSP).....	56

LIST OF FIGURES

	<u>Page</u>
Figure 1.1 : Molecular structures of several conjugated polymers.	3
Figure 1.2 : Molecular orbital (MO) diagram.	6
Figure 1.3 : Classification of materials, and schematic of valence and conduction bands and band gap.	7
Figure 1.4 : Oxidative doping of thiophene	9
Figure 1.5 : Poly(3,4-alkylenedioxythiophene)s (PXDOT)s.	17
Figure 1.6 : Poly(3,4-ethylenedioxythiophene)	17
Figure 1.7 : Poly(N-Phenylsulfonyl pyrrole).	18
Figure 1.8 : SEM image of conductive polymer coated SCFME.	19
Figure 1.9 : Sinusoidal current response in a linear system.	22
Figure 1.10 : Nyquist plot with impedance vector.	24
Figure 1.11 : Bode plot with one time constant.	25
Figure 1.12 : An equivalent circuit representing each component at the interface and in the solution during an electrochemical reaction is shown for comparison with the physical components	26
Figure 1.13 : Transmission line circuit model.	27
Figure 1.14 : Infrared spectrum bands for general substitutions.	31
Figure 1.15 : Electronic transitions.	32
Figure 1.16 : Schematic diagram of atomic force microscope	34
Figure 1.17 : Schematic AFM contact probe.	35
Figure 2.1 : A geometry of one compartment-3 electrode cell.	38
Figure 3.1 : Cyclic voltammogram of electrogrowth of 10 mM PSP 5 mM EDOT in 0.1 M NaClO ₄ /ACN at 30 mV/s, 10 cycle on SCFME. Inset: CV of monomer free of Poly(EDOT-co-PSP) film in 0.1M NaClO ₄ /ACN. ...	42
Figure 3.2 : Cyclic voltammogram of electrogrowth of 10 mM PSP 1.66 mM EDOT in 0.1 M NaClO ₄ /ACN at 30 mV/s, 10 cycle on SCFME. Inset: CV of monomer free of Poly(EDOT-co-PSP) film in 0.1M NaClO ₄ /ACN.	43
Figure 3.3 : Cyclic voltammogram of electrogrowth of 10 mM PSP 1 mM EDOT in 0.1 M NaClO ₄ /ACN at 30 mV/s, 10 cycle on SCFME. Inset: CV of monomer free of Poly(EDOT-co-PSP) film in 0.1M NaClO ₄ /ACN. ...	43
Figure 3.4 : Cyclic voltammogram of electrogrowth of 10 mM PSP 0.5 mM EDOT in 0.1 M NaClO ₄ /ACN at 30 mV/s, 10 cycle on SCFME. Inset: CV of monomer free of Poly(EDOT-co-PSP) film in 0.1M NaClO ₄ /ACN	44
Figure 3.5 : Plot of anodic and corresponding cathodic peak current density vs. the scan rate of the Poly(EDOT-co-PSP) films in different electrolyte solutions.	45
Figure 3.6 : Chemical structure of Poly(EDOT-co-PSP).	46
Figure 3.7 : Ex-situ FTIR-ATR spectrum of Poly(EDOT-co-PSP) and PEDOT powders obtained via chronoamperometry method on steel plates.	46

Figure 3.8 : Comparison of FTIR-ATR peak area ratios to understand the presence of PSP in the copolymer.....	48
Figure 3.9 : Ex-situ spectroelectrochemical measurements (UV-Vis) of different mole fractions of EDOT-PSP oligomers.....	49
Figure 3.10 : Ex-situ spectroelectrochemical measurements (UV-Vis) of EDOT and EDOT-PSP	49
Figure 3.11 : Nyquist plots of Poly(EDOT-co-PSP)s electrografted on SCFMEs correlated with the calculated data from the equivalent circuit modlling $R(C(R(Q(RW))))$	51
Figure 3.12 : Bode phase plots of Poly(EDOT-co-PSP)s electrografted on SCFMEs correlated with the calculated data from the equivalent circuit modlling $R(C(R(Q(RW))))$	51
Figure 3.13 : Bode magnitude plots of Poly(EDOT-co-PSP)s electrografted on SCFMEs correlated with the calculated data from the equivalent circuit modlling $R(C(R(Q(RW))))$	52
Figure 3.14 : Low frequency capacitances (obtained from EIS) and film resistances for different mole fractions of Poly(EDOT-co-PSP) and PEDOT.....	53
Figure 3.15 : Scheme of the equivalent circuit model.	54
Figure 3.16 : Scheme of the interface between copolymer film coated electrode and supporting electrolyte solution	54
Figure 3.17 : SEM images of (a) Poly(EDOT-co-PSP) and (b) PEDOT which show the difference between pore formation.....	55
Figure 3.18 : SEM image of athe copolymer coated SCFME with a mole fraction of PSP of 0.66.	57
Figure 3.19 : SEM image of athe copolymer coated SCFME with a mole fraction of PSP of 0.86.	57
Figure 3.20 : SEM image of athe copolymer coated SCFME with a mole fraction of PSP of 0.90.	58
Figure 3.21 : SEM image of athe copolymer coated SCFME with a mole fraction of PSP of 0.95	58
Figure 3.22 : AFM topographies of Poly(EDOT-co-PSP) coated silicon wafer.....	59

ELECTROCHEMICAL COPOLYMERIZATION OF EDOT AND N-PHENYLSULFONYL PYRROLE: MORPHOLOGIC, SPECTROSCOPIC, ELECTROCHEMICAL CHARACTERIZATIONS

SUMMARY

The preparation, characterization and application of electrochemically active conducting polymers are challenging research activity in electrochemistry. Electrochemical polymerization represents a widely employed route for the synthesis of some important classes of conjugated polymer such as polythiophene (PTh).

Carbon fiber is a polymer which is a form of graphite. Graphite is a form of pure carbon. In graphite the carbon atoms are arranged into big sheets of hexagonal aromatic ring. Porous carbon is the most frequently selected electrode material which offers a large surface area and very well polarization due to porosity which makes porous carbon is one of the most promising electrode material for supercapacitor application.

Carbon fiber micro electrode shows superior performance in electrochemical studies due to its micron size cylindrical structure. It has a disposable character having a new surface area at each uses compared to Pt or Au electrodes.

In this study, 3,4-Ethylenedioxythiophene and N-phenylsulfonyl pyrrole electrocopolymerized in various mole fractions with a cyclic voltammetry, their characterization, ex-situ spectroelectrochemistry and EIS were investigated.

Electropolymerization process was performed on the SCFMEs by cyclic voltammetry at a scan rate of 30 mV/s at (-0.8 – 1.3)V for the monomers using 10 cycles in 0.1M NaClO₄/ACN.

Ex-situ spectroelectrochemistry of Poly(EDOT-co-PSP) films were studied on the potentiodynamically deposited steel plates. FTIR-ATR measurements indicate that the inclusion of PSP into the copolymer structure, especially for the mole fraction of PSP of 0.95. Oligomers of copolymers dissolved in electrolyte solution during electrocopolymerization resulting colored solutions, measured by UV-Vis spectrophotometry.

EIS measurements were performed at open circuit potential range of 0.01Hz-100kHz (application of amplitude of 10 mV) for Poly(EDOT-co-PSP). For the mole fraction of PSP of 0.86, highest low frequency capacitance value (C_{LF}) was obtained by using EIS. The shape of the plot has a good agreement with the corresponding CV of the polymer film in monomer free solution.

The electrochemical parameters of the Poly(EDOT-co-PSP) / Electrolyte system were evaluated by employing ZSimpWin (version 3.10) software from Princeton Applied Research. Variation of the solution resistance (R_s), charge transfer resistance (R_{CT}), double layer capacitance (C_{DL}), film resistance (R_F), Warburg diffusion constant and constant phase element (CPE) in different mole fractions of Poly(EDOT-co-PSP) film were investigated via equivalent circuit models.

Morphology of coatings for different mole fractions were studied. The SEM pictures show a cauliflower-like morphology for Poly(EDOT-co-PSP) films on SCFMEs.

3,4-ETİLENDİOKSİTİYOFEN VE N-FENİLSULFONİL PİROLÜN ELEKTROKİMYASAL KOPOLİMERİZASYONU: MORFOLOJİK, SPEKTROSKOPİK, ELEKTROKİMYASAL KARAKTERİZASYONU

ÖZET

Elektrokimyasal olarak aktif olan konjuge polimerlerin sentezlenmesi, karakterizasyonu ve uygulama alanları günümüzde çalışılan en popüler elektrokimya konularıdır. Elektrokimyasal polimerizasyon politiyofen gibi önemli iletken polimerlerin sentezinde ve karakterizasyonunda kullanılan en önemli yöntemdir.

Karbon fiber bir çeşit grafit formu olarak tanımlanırken, grafit ise saf karbon olarak adlandırılabilir. Grafit yapısında karbon atomları düzlemsel yapı üzerinde hegzagonal halkalar halinde bulunmaktadır. Porlu yapıya sahip karbon, geniş yüzey alanı sağlama ve iyi polarize olması açısından süper kapasitör uygulamalarında en çok tercih edilen elektrot malzemesidir.

Karbon fiber mikro elektrotlar sahip oldukları mikron boyutundaki silindirik yapıları altın ve platindeki gibi yüzey temizleme işlemi gerektirmeden tek kullanımlık olarak hazırlanması açısından elektrokimyasal polimerizasyon işlemlerinde tercih edilmektedir. Ayrıca birçok durumda metal elektrotlara nazaran daha iyi sonuçlar verdiği saptanmıştır.

Bu çalışmada, farklı mol fraksiyonlarındaki 3,4-Etilendioksitiyofen (EDOT) ve N-Fenilsülfonil pirol (PSP), döngülü voltametri ile elektrokimyasal olarak kopolimerleştirilmiştir. Bu filmlerin karakterizasyonu, ex-situ spektroeletrokimyası ve elektrokimyasal empedans spektroskopisi incelenmiştir.

Elektrokimyasal proses, tek karbon fiber mikro elektrot (TKFME) üzerinde döngülü voltametri ile, 30 mV/s tarama hızında, (-0,8 - 1,3)V potansiyel aralığında, 0,1M NaClO₄/ACN içinde 10 döngü uygulanarak gerçekleştirilmiştir.

Poli(EDOT-ko-PSP) filmlerinin ex-situ spektroeletrokimyası, potensiyodinamik olarak çelik tabaka üzerinden kazınarak incelenmiştir. FTIR-ATR ölçümlerinin sonuçlarına göre, PSP'nin kopolimer yapısına girişi, PSP'ye ait mol fraksiyonunun 0,95 olduğu durumda belirgin şekilde gözlenmiştir. Elektrokopolimerizasyon sırasında kopolimerin elektrolit çözeltisi içinde çözünmüş oligomerleri çözeltiyi renklendirmiştir. Bu çözeltinin UV-Vis ölçümü alınmış ve oligomer davranışı incelenmiştir.

Elektrokimyasal empedans ölçümleri farklı mol fraksiyonlarına sahip poli(EDOT-ko-PSP) kopolimerleri için 100kHz-10mHz aralığında açık devre potansiyelinde ve monomer içermeyen elektrolit ortamında 10mV potansiyelde ölçülmüştür. $X_{PSP}=0,86$ olduğu durumda en yüksek, düşük frekans kapasitans değeri (C_{LF}) elektrokimyasal empedans spektroskopisi ile elde edilmiştir. Monomer içeren çözeltinin döngülü voltamogramının şekli, kopolimer filmin monomer içermeyen elektrolit ortamındaki döngülü voltamogramına benzer bir eğilim göstermiştir.

Poli(EDOT-ko-PSP) / Elektrolit sisteminde elektrokimyasal parametreler Princeton Applied Research için uygulanan ZSimpWin (versiyon 3.10) yazılımında gerçekleştirilmiştir. Poli(EDOT-ko-PSP) filmlerinin çözelti dirençlerinin çeşitliliği, çift tabaka kapasitans, film resistansı, yük transfer resistansı, Warburg difüzyon sabiti ve sabit faz elementi farklı mol fraksiyonlarındaki kopolimer filmler için bir eşdeğer devre modeli üzerinde incelenmiştir.

Farklı mol fraksiyonlarına sahip poli(EDOT-ko-PSP) film kaplamalarının görünümü SEM resimleri ile görülmektedir. SEM resimleri, TKFME üzerinde poli(EDOT-ko-PSP) filmlerinin karnıbahar görünümünde olduğunu göstermiştir.

1. INTRODUCTION

1.1 Conductive Polymers

Conductive polymers (CPs) have attracted considerable interest in recent years because of their potential applications in different technologies, for example, in electronic displays, smart windows, sensors, catalysis, redox capacitors, actuators and in secondary batteries [1-5]. In 1958, polyacetylene was first synthesized by Natta as a black powder. This was found to be a semi-conductor with a conductivity between 7×10^{-11} to $7 \times 10^{-3} \text{ S.m}^{-1}$, depending upon how the polymer was processed and manipulated. This compound remained a scientific curiosity until 1967, when a postgraduate student of Hideki Shirakawa at the Tokyo Institute of technology was attempting to synthesize polyacetylene, and a silvery thin film was produced as a result of mistake. It was found that 1000 times too much of the Ziegler-Natta catalyst, $\text{Ti}(\text{O-n-But})_4 - \text{Et}_3\text{Al}$, had been used. Further investigations, initially aimed to produce thin films of graphite, showed that exposure of this form of polyacetylene to halogens increased its conductivity a billion fold. Undoped, the polymer was silvery, insoluble and intractable, with a conductivity similar to that of semiconductors. When it was weakly oxidized by compounds such as iodine it turned a golden color and its conductivity increased to about 10^4 S.m^{-1} .

Conducting polymers (CPs) are an exciting new class of electronic materials, which have attracted rapidly increasing interest since their discovery in 1979 [6]. CPs have the potential of combining the high conductivities of pure metals with the processability, corrosion resistance and low density of polymers [7], electrochromic displays [8], electromagnetic shielding [9], sensor technology [10], non-linear optics [11] and molecular electronics[12].

Polyheterocycles were found to be much more air stable than polyacetylene, although their conductivities were not so high, typically about 100 S.cm^{-1} . By adding various side groups to the polymer backbone, derivatives which were soluble in various solvents were prepared. Other side groups affected properties such as their color and their reactivity to oxidizing and reducing agents. Electrochemical polymerization represents a widely employed route for the synthesis of some important classes of conjugated polymers such as polypyrrole (PPy) and polythiophene (PTh). During the past two decades these materials have been the focus of considerable interest motivated by both fundamental problems posed by their structure and electrical properties and their multiple potential technological applications [13] including transparent electrode materials [14]. Conducting polymers can be prepared via chemical or electrochemical polymerization [15]. Electrochemical synthesis is rapidly becoming the preferred general method for preparing electrically conducting polymers because of its simplicity and reproducibility. The advantage of electrochemical polymerization is that the reactions can be carried out at room temperature. By varying either the potential or current with the time the thickness of the film can be controlled [16]. Films of electronically conducting polymers are generally obtained onto a support electrode surface by anodic oxidation (electropolymerization) of the corresponding monomer in the presence of an electrolyte solution. Different electrochemical techniques can be used including potentiostatic (constant potential), galvanostatic (constant current), and potentiodynamic (potential scanning i.e., cyclic voltammetry) methods. Electrically conductivity is achieved in the film of conducting polymer by oxidation (p-doping) or reduction (n-doping), followed respectively by the insertion of anionic or cationic species [17]. The π -electron system along the polymer backbone, which confers rigidity and the cross linking points between polymer chains, make conducting polymers insoluble, infusible and poorly processable.

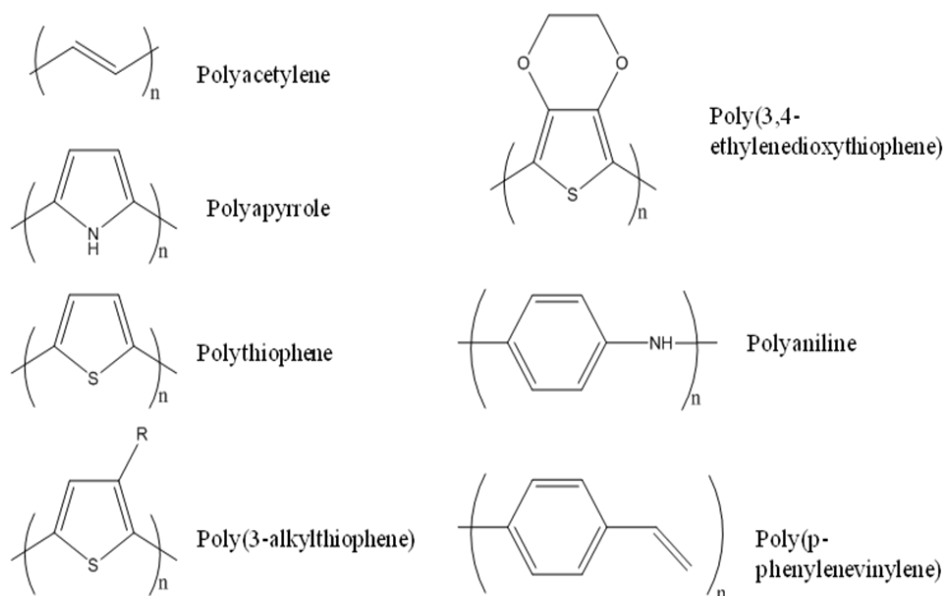


Figure 1.1: Molecular structures of several conjugated polymers

In view of the wide spectrum of potential applications, it is clear that a further control of the electropolymerization conditions, use of different substrates and stability of resulting polymer can contribute to extend the scope of the technological applications of conducting polymers as thin films. The electrografting of a range of copolymers with various monomer concentrations have been recently examined using carbon fibers as the electrode [11-23]. The preparation of a range of conducting polymers, i.e. carbazole has also been described. Electrografting and relationship between the polymerization parameters and the surface properties of the electrodes are established [24].

1.1.1 Use of conducting polymers

Numerous applications have been demonstrated and proposed for conjugated polymers. Some of the present and potential commercial applications of these systems are listed below [25-26].

- Storage batteries, super capacitors, electrolytic capacitors and fuel cells
- Sensors (biosensors and chemical sensors)
- Ion-specific membranes
- Ion supply / exchange devices (drug and biomolecule release)
- Electrochromic displays (ECDs) (electromagnetic shutters)

- Corrosion protection
- Transparent conductors
- Mechanical actuators (artificial muscles)
- Gas separation membranes
- Conductive thermoplastics
- Microwave weldable plastics
- Electromagnetic interference (EMI) shielding
- Aerospace applications (lightning strike protection, microwave absorption / transmission)
- Conductive textiles
- Antistatic films and fibers (photocopy machines)
- Conductor / insulator shields
- Neutron detection
- Photoconductive switching
- Conductive adhesives and inks
- Electronics (conductor feedthroughs)
- Non-linear optics
- Electronic devices

This list can be divided into three main classes based mainly on function and redox state. Firstly, applications that utilize the conjugated polymer in its neutral state are often based around their semi-conducting properties, as in electronic devices such as field effect transistors or as the active materials in electroluminescent devices. Secondly, the conducting forms of the polymers can be used for electron transport, electrostatic charge dissipation, and as EMI-shielding materials. These first two types of applications can be viewed as static applications (as the polymers do not change their electronic state during use). The final area of the applications is based around those that use the ability of the polymers to redox switch between charge states. These include their use as battery electrode materials, electrochromic materials, and in ion release devices and biosensors.

Conducting polymers show interesting electrochromic properties. For instance, depending on the structures and substituents, polymer films show different colors and different properties, such as cathodic or anodic coloration, multi-coloration, etc. The remarkable advances in electrochromic performance can be viewed from several fronts. First, the range of colors now available effectively spans the entire visible spectrum [27] and also extends through the near and mid-infrared regions. This is due to the ability to synthesize a wide variety of polymers with varied degrees of electron-rich character and conjugation. For example, a fine adjustment of the band gap, and consequently of the color, is possible through modification of the structure of the polymer via monomer functionalization, copolymerization [28], and the use of blends, laminates and composites [29-30]. Second has been the marked increase in device lifetimes. The key to this is control of the degradation processes within the polymeric materials (by lowering the occurrence of structural defects during polymerization) and the redox systems [31-32]. Third the polymer based ECDs have achieved extremely fast switching times of a few hundreds of milliseconds for large changes in optical density. This fast switching is attributed to a highly open morphology of electroactive films, which allows for fast dopant ion transport [33]. Other beneficial properties of polymers are outstanding coloration efficiencies [34] along with their general process ability.

1.1.2 Band gap theory

All of these systems share one common structural feature, namely a rigid nature brought about by sp^2 carbon-based backbone. The utilization of the conjugated constructions affords polymer chains possessing extended π -systems, and it is this feature alone that separates CPs from their other polymeric counterparts. Using this generic, lowest energy (fully bonding) molecular orbital (MO) representation as shown by the π -systems model, the picture of primary concern that is generated by these networks consists of a number of π and π^* levels (Figure 1.2)

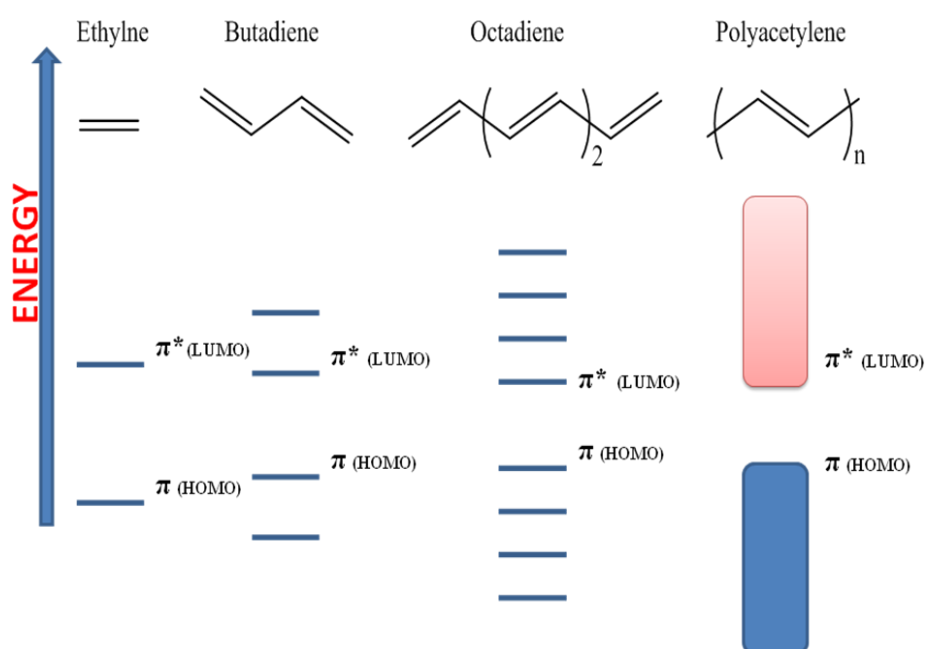


Figure 1.2: Molecular orbital (MO) diagram

The electrical properties of any material are a result of the material's electronic structure that CP's form bands through extensive molecular orbital overlap leads to the assumption that their electronic population are the chief determinants of whether or not a material is conductive.

Metals are material that possess partially-filled bands, and this characteristic is the key factor leading to the conductive nature of this class of materials. Semiconductors, on the other hand, have filled (valence bands) and unfilled (conduction bands) bands that are separated by a range of forbidden energies (known as the band-gap).

The conduction band can be populated, at the expense of the valence band, by exciting electrons (thermally and/ or photochemically) across this band gap. Insulators possess a band structure similar to semiconductors except here the band gap is much larger and inaccessible under the environmental conditions employed (Figure 1.3).

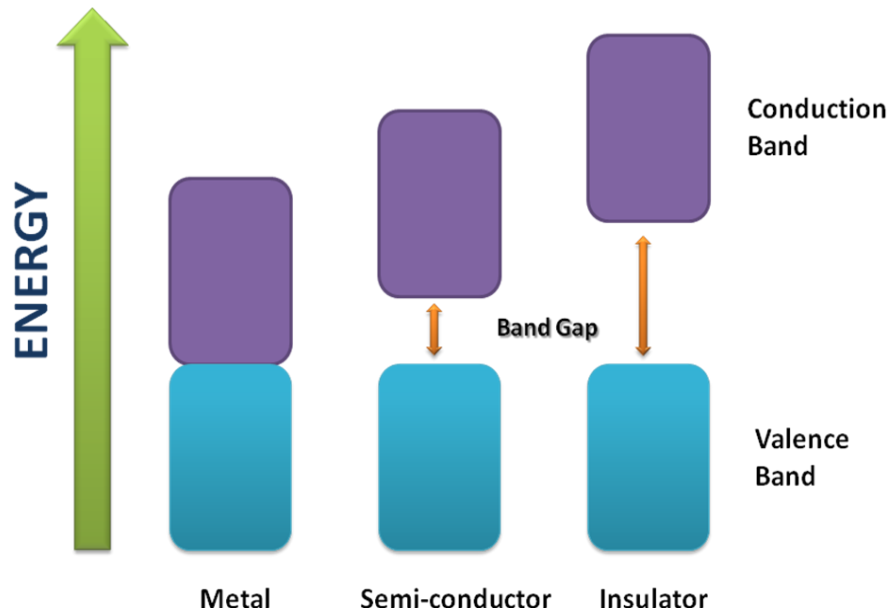


Figure 1.3: Classification of materials, and schematic of valence and conduction bands and band gap

For electrical conductivity to occur, electrons must have a vacant place (a hole) to move to and occupy. When bands are completely filled or empty, conduction can not occur. Metals are highly conductive because they possess unfilled bands. Semiconductors possess an energy gap small enough that thermal excitation of electrons from the valence to the conduction bands is sufficient for conductivity however, the band gap in insulators is too large for thermal excitation of electrons across the band gap.

1.1.3 Doping and electrical conductivity

In the late 1970s Heeger and McDiarmid found that polyacetylene produced by Shirakawa's method exhibited a 12 order of magnitude increase in electrical conductivity when exposed to oxidizing agents. The diffuse nature of the extended π -system readily allows electron removal from, or injection, into the polymer. The term doping being used to describe polymer oxidation and reduction, respectively. Doping in regards to semiconductors is quite different as it is a very distinct process carried out at low levels (<1%) as compared to CP doping (usually 20-40%). However, the manner by which doping transforms a neutral CP into a conductor remained a mystery for many years.

Electron Paramagnetic Resonance (EPR) studies have shown that both the neutral and heavily doped CPs possess no net spin, interpreted as no unpaired electrons, while moderately doped materials were discovered to be paramagnetic in nature. Conductivity experiments showed that it was the "spin-less", heavily-doped form that is the most conductive for a given CP. Such behavior marks an abrupt departure from simple band theory, which centers around spin-containing charge carriers.

Polyacetylene turns out to be a special case when considering its neutral and doped forms. Comparison of the two neutral forms, reveals them to be structurally identical, and thus, their ground states are degenerate in energy. Two successive oxidation on one chain could yield radical cations that, upon radical coupling, become non-associated charges termed positive "solitons".

In contrast to polyacetylene, the other CPs have non-degenerate ground states (i.e., they do not possess two equivalent resonance forms, and thus, do not show evidence of solitons formations). In this instance, the oxidation of the CP is believed to result in the destabilization (raising of the energy) of the orbital from which the electron is removed. This orbital's energy is increased and can be found in the energy region of the band gap as shown. Initially, if only one electron per level is removed a radical cation is formed and is known as a polaron. Further oxidation removes this unpaired electron yielding a dicationic species termed a bipolaron.

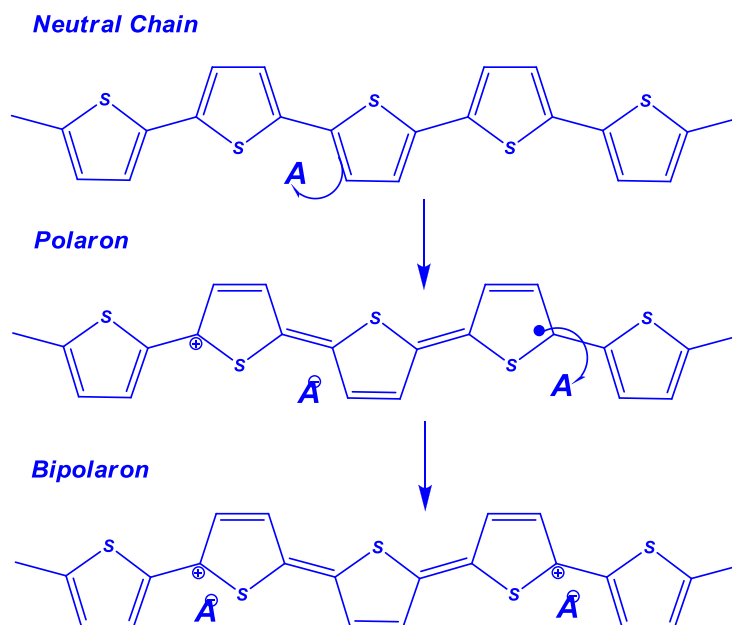


Figure 1.4: Oxidative doping of thiophene (A^{\ominus} : dopant)

High dopant concentrations create a bipolaron-rich material and eventually leads to band formation of bipolaron levels. Such a theoretical treatment, thereby, explains the appearance, and subsequent disappearance of the EPR signal of a CP with increased doping as the spin-less bipolaronic state.

Contrary to polyacetylene's independent charges, the bipolaron unit remains intact and the entire entity propagates along the polymer chain. In the case of unsubstituted polythiophene, the bipolaronic unit is believed to be spread over six to eight rings. This bipolaron length is by no means an absolute number as different polymer backbone and substituent types yield various lengths.

While this general model of charge carrier generations has developed over the years, it is not without conjecture. As one alternate possibility, the presence of diamagnetic π -dimers, resulting from the combination of cation radicals, has been proposed. Much of the basis of these theories comes from investigations into the structural and electronic properties of small conjugated molecules.

1.1.4 Optical properties

Doping also brings about radical changes in a CPs optical properties. For instance, neutral polythiophene films are red in color, while doped polythiophene is blue in color. A broad variety of color changes that can be structurally controlled have been observed for the CPs in changing between their respective redox state. These optical changes are a consequence of polaronic levels and bipolaron bands residing in the band gap. While the neutral polymer only has its characteristic π - π^* transition, several new transitions are necessarily lower and result in the polymer having red-shifted absorptions. While the altering of a CPs optical properties can be readily accomplished via chemical means, electrochemical doping is attractive from an applications standpoint, and these polymers provide a new family of electrochromic materials.

1.2 Electrochemical Polymerization

Electrochemical synthesis utilizes the ability of a monomer to be self-coupled upon irreversible oxidation (anodic polymerization) or reduction (cathodic polymerization). While this method does not always produce materials with well-defined structures (other polymerization methods will be discussed), electropolymerization, nonetheless, is a rather convenient alternative, avoiding the need for polymer isolation and purification.

In an electrochemical polymerization, the monomer, dissolved in an appropriate solvent containing the desired anionic doping salts, is oxidized at the surface of an electrode by application of an anodic potential (oxidation). The choice of the solvent and electrolyte is of particular importance in electrochemistry since both solvent and electrolyte should be stable at the oxidation potential of the monomer and provide an ionically conductive medium [35].

As a result of the initial oxidation, the radical cation of the monomer is formed and reacts with other monomers present in solution to form oligomeric products and then the polymer. The extended conjugation in the polymer results in a lowering of the oxidation potential compared to the monomer. Therefore, the synthesis and doping of the polymer are generally done simultaneously.

The anion is incorporated into the polymer to ensure the electrical neutrality of the film and, at the end of the reaction, a polymeric film of controllable thickness is formed at the anode. The anode can be made of a variety of materials including platinum, carbon fiber, gold, glassy carbon and indium tin oxide (ITO) coated glass. The electropolymerization is generally achieved by potentiostatic (constant potential) or galvanostatic (constant-current) methods. Potentiodynamic techniques such as cyclic voltammetry corresponds to a triangular potential waveform applied at the surface of the electrode [36].

1.2.1 Chronoamperometry

Chronoamperometric method is used to measure the current as a function of time, is a method of choice to study the kinetic of polymerization and especially the first steps [37]. As a potential step is large enough to cause an electrochemical reaction is applied to an electrode, the current changes with time. The study of this current response as a function of time is called chronoamperometry (CA). CA is a useful tool for determining diffusion coefficients and for investigating kinetics and mechanisms. Unlike CV, CA can yield this information in a single experiment.

In CA, the current is monitored as a function of time. It is important to note that the basic potential step experiment is CA; that is, during the experiment, the current is recorded as a function of time. However, after the experiment, the data can also be displayed as charge as a function of time (the charge is calculated by integrating the current). Hence, chronocoulometry data can be obtained.

Chronoamperometry is an electrochemical technique in which the potential of working electrode is stepped and the resulting current from faradaic processes occurring at the electrode is monitored as a function of time.

The current-time curve is described as Cottrell equation.

$$I = nFACD^{1/2}\pi^{-1/2}t^{-1/2}$$

where: n = number of electrons transferred/molecule

F = Faraday's constant (96,500 C mol⁻¹)

A = electrode area (cm²)

D = diffusion coefficient (cm²s⁻¹)

C = concentration (mol cm^{-3})

1.2.2 Chronopotentiometry

Chronopotentiometric method is used to measure the potential as a function of time. For this technique constant current is applied for elapsed time, than uniformity of coated structure could be decided by checking the linearity of the potential difference with the time. Chronopotentiometry is also named as galvanostatic method and reaction could either be done via galvanostat. Common applications of the galvanostat include constant current stripping potentiometry and constant current electrolysis. One advantage of all constant current techniques is that the ohmic drop due to solution resistance is also constant, as it is equal to the product of the current and the solution resistance.

1.2.3 Factors affected the electropolymerization

1.2.3.1 Monomer substitution

Presence of alkyl group gives solubility to copolymers obtained both chemically and electrochemically [38]. The substituents on the Nitrogen atom can influence the conductivity: the greater the steric interaction between repeat units is the weaker the conductivity will be. The influence of N-substitution on the electropolymerization characteristics was examined by Waltman [39].

The polymer yield and the rate of oxidation were found the decrease as the size of the alkyl group increases. Bonding large substituents to the Nitrogen atom or to the β -carbon stabilizes to cation radical without stopping the polymerization [40]. If this intermediate is too stable it can diffuse into the solution and form soluble products. As a result, the yield and the molecular weight of the polymer will be low.

1.2.3.2 Effect of the electrolyte

The choice of an electrolyte is made by considering its solubility and nucleophilicity. Moreover the anion oxidation potential should be higher than the monomer. The nature of the anion has an impact on the quality of the film produced which depends on the hydrophobic character of the anion and the interactions between the polymer and the anion. For instance, Kassim et al. [41] have shown that in aqueous solution, the utilization of a large aromatic sulfate anion gives stable conducting polymers with better mechanical properties than when a perchlorate anion is used because of their hydrophobic interaction with water, one of roles played by these organic anions is to orient polymer chain parallel to the electrode surface. This chain orientation increases the order in the polymer structure [42]. On the other hand, anion nucleophilicity interferes with the reaction by increasing the formation of soluble products. The polymer of the highest conductivity is produced when elevated concentrations of electrolyte are used [43].

1.2.3.3 Effect of cation

The copolymer possessing cation recognition properties have been subjected to a sustained interest in recent years. The electrochemical properties were analyzed in the presence of the different alkali cations (Li^+ , Na^+ , K^+). In each case addition of incremental amounts of cation produces a positive shift of the anodic peak potential and a decrease of electroactivity [44]. The size of the cation can have an influence on the polymer conductivity. It is shown that the larger cation, the lower conductivity of the polymer [45].

1.2.3.4 Effect of the solvent

The solvent used for electropolymerization is an important factor governing not only the quality of the conducting polymer obtained, but also its conductivity, morphology and subsequently the electrochemical behavior. The solvent must minimize the nucleophilicity reactions. Among these solvents, ACN is the most commonly used. Nucleophilic solvents like DMF or DMSO do not allow polymer formation to occur unless a protic acid, like p-toluenesulfonic acid is added [46]. In ACN, the addition of small quantities of water has a big influence on the kinetics of the reaction and the properties of the polymer formed [47]. This effect is due to the stabilization of the cation radical intermediate by the water molecules which have a larger polarity than ACN.

Film formation is influenced by the strength of the interactions between the solvent and the cation radicals. The basicity of the solvent is the principal factor affecting the selectivity in polymer formation. On the other hand, the solvent polarity will affect the strength of the interactions between the solvent and the electrolyte anions.

Ko et al. have studied the morphology and the film properties in aqueous and nonaqueous solution (in the case of ACN) [48]. They have found that the film prepared in ACN are more homogeneous and better conductors as compared to the polymers prepared in aqueous solution undergo attack by water molecules during reaction which is responsible for their irregular morphology and their weak properties. Unsworth et al. have shown that the adsorption of oxygen gas formed during water oxidation is a source of surface defects in the polymer [49].

In dried ACN, acid catalyzed formation of a pyrrole trimer having a broken conjugation yields a partly conjugated and poorly conductive PPy which passivates the electrode after deposition. The favorable effect of water comes from its stronger basicity than pyrrole and therefore it has the ability to capture the protons released during the electropolymerization. This prevents the formation of the trimer and thus avoids the passivation of the electrode.

Solvent retention within the polymer matrix, retention of solvent affinity sites, are important factors. Thus, for instance, several polypyrrole derivatives, when electropolymerized in ACN or PC will show a well electrochemically cycle well only in the solvent of electropolymerization [50]. Solvents may also be too nucleophilic: besides its high solvation capability for even doped CPs, DMF is also poor electropolymerization solvent due to high nucleophilicity; if this is reduced with addition of protic solvents, electropolymerizations are observed [51].

1.2.3.5 Effect of the temperature

Electropolymerization temperature has a substantial influence on the kinetics of polymerization as well as on the conductivity, redox properties and mechanical characteristics of the films. Films prepared at lower temperatures have a more rugged appearance and poorer adhesion than those prepared at higher temperatures [52].

- a) A conjugated polymer's conductivity decreases with decreasing temperature.
- b) A semiconductor's DC conductivity decreases with decreasing temperature, remains finite at low temperatures.
- c) A metal DC conductivity increases slightly with decreasing temperature [53].

1.2.3.6 Scan rate dependencies

One of the first characteristics of CV of a CP film that one searches for is the dependence of the peak current (I_p) on the scan rate (v). According to well established electrochemical treatments, for a behavior dominated by diffusion effects, I_p is proportional to $v^{1/2}$, whilst for a material localized on an electrode surface, such as CP film, I_p is proportional to v . For most CP films the latter case obtains, thus indicating surface localized electroactive species. As more detailed analysis shows, however, this is so only for CP films that are not inordinately thick (which most are not), not inordinately compact (which most are not), and not doped with very large dopant ions which have inordinately small diffusion coefficients (which most dopants do not). If any of the latter conditions prevail, however i.e., wherever dopant diffusion effects can predominate I_p can be proportional to $v^{1/2}$, as in the case of copolymer.

1.2.4 PXDOT derivatives

Due to its high oxidation potential, thiophene itself is difficult to polymerize electrochemically. However, upon alkyl substitution the monomer oxidation potential is lowered to an easily accessible range, which has resulted in the extensive study of poly(3-methylthiophene) and poly(3-alkylthiophene) [54].

Substitution at the 3- and 4- positions of thiophene prevents the occurrence of α - β and β - β coupling during electropolymerization, yielding more ordered polymers with longer conjugation lengths. Initially, the synthesis of 3,4-disubstituted polythiophenes was carried out with the goal of stabilizing the oxidized form, as well as providing solubility and processability [55].

While these substituents do lower the oxidation potential and stabilize the oxidized form of the polymers to nucleophilic attack, they also lead to severe steric interactions that distort the π -conjugated system [56] decreasing the degree of conjugation and lowering the conductivity. To overcome this drawback, poly(3,4-cycloalkylthiophenes) were synthesized, and it was demonstrated that carbocycles at the 3- and 4- positions reduced the steric hindrance, especially in the case of poly(3,4-cycloalkylthiophenes). This strategy was taken a step further and the methylene adjacent to the heterocycle was replaced by a heteroatom making the oxidized form even more stable with less steric distortion. As a result, polythiophenes carrying 3,4-dialkoxy and 3,4-alkylenedioxy substituents exhibit the most pronounced stability.

Jonas et al. [57] were the first to anodically polymerize a member of the 3,4-alkylenedioxythiophene family, 3,4-ethylenedioxythiophene. The most intensive research has focused on the PEDOT parent as it has been successfully commercialized by AGFA-Gevaert N.V. and Bayer AG. Using EDOT as the core linkage, materials have been prepared in which the conductivity ranges from less than 10^{-1} Scm^{-1} . Furthermore, their optical properties can be varied over a broad range as evidenced by the electronic bandgap, which ranges from less than 1.0 eV to 2.4 eV.

As a class of conducting and electroactive polymers that can exhibit high and quite stable conductivities, a high degree of optical transparency as a conductor, and the ability to be rapidly switched between conducting doped and insulating neutral states, poly(3,4-alkylenedioxythiophene)s (PXDOTs) (Figure 1.5), have attracted attention across academia and industry.

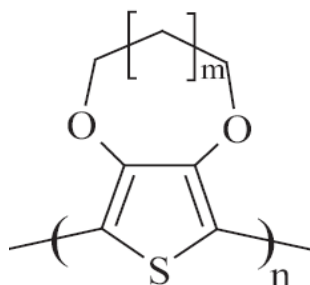


Figure 1.5: Poly(3,4-alkylenedioxythiophene)s (PXDOTs)

Since both chemically and electrochemically prepared PXDOT is insoluble and unprocessable, intensive research has been carried out to synthesize PXDOT derivatives that would overcome this problem.

1.2.5 PEDOT

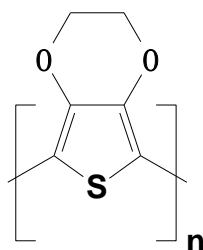


Figure 1.6: Poly(3,4-Ethylenedioxythiophene) (PEDOT)

Poly(3,4-ethylenedioxythiophene) (PEDOT) is one of the π -conjugated conducting polymer. In particular, PEDOT is an interesting material because of its good thermal and chemical stability, low oxidation potential and a high electrical conductivity in the p-doped state (easily up to 550 Scm^{-1}) [58]. Conducting PEDOT films are investigated for use as supercapacitors [59], antistatic materials [60], electrochromic devices [61-64] and biosensors [65]. One method to synthesize PEDOT is electropolymerization of 3,4-ethylenedioxythiophene (EDOT). Most of the studies on the electropolymerization of EDOT and electrochemical characterization of PEDOT have been carried out in organic solution [62,66-67]. However, aqueous

solutions have also been used. The solvent, the electrode, supporting electrolyte, applied polymerization potential and applied electropolymerization method are the important factors on PEDOT film which was synthesized by electrochemical method [68]. The electrical properties of PEDOT result from its polymeric structure. The electron donating Oxygen atoms in 3- and 4- positions not only reduce the oxidation potential of the aromatic ring, but also prevent α,β -coupling during the polymerization. The ethylene bridges makes steric distortion effects minimum resulting in a high stereoregularity of the polymer chain, thus good π -conjugation is guaranteed [69].

In the last years the excellent properties of PEDOT have been combined with some typical conducting polymers with promising potential applications to produce new copolymers with properties intermediate between two. So far, copolymers of EDOT with pyrrole [70-71], N-methylpyrrole [72], thiophene [73], bithiophene [74], 3-methylthiophene [75], N-ethyl carbazole [76], N-substituted carbazole [76], indole[77] have been reported.

1.2.6 N-Phenylsulfonyl pyrrole

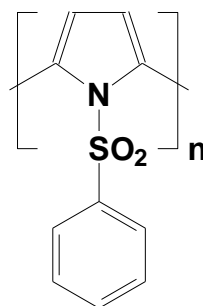


Figure 1.7: Poly(N-phenylsulfonyl pyrrole)

The chemical synthesis of N-Phenylsulfonyl pyrrole (PSP) was reported in [78] for the purposes of implementing a gas sensor. Additionally, N-phenyl sulfonyl-1H-pyrrole-3-sulfonyl chloride was synthesized in acetonitrile by using chronosulphonic acid [79].

1.3 Carbon Fiber Microelectrodes

Carbon due to different allotropes (graphite, diamond, ly.fullerens / nanotubes), various microtextures (more or less ordered) owing to the degree of graphitization, a rich variety of dimensionality from 0 to 3D and ability for existence under different forms (from powders to fibers, foams, fabrics and composites) represents a very attractive material for electrochemical applications , especially for storage of energy. Carbon electrode is well polarizable; however, its electrical conductivity strongly depends on the thermal treatment, microtexture, hybridization and content of heteroatoms. Additionally, the amphoteric character of carbon allows use of the rich electrochemical properties of this element from donor to acceptor state. Apart from it, carbon materials are environmentally friendly. During the last years a great interest has been focused on the application of carbons as electrode materials because of their accessibility and easy processability and relatively low cost. They are chemically stable in different solutions (from strongly acidic to basic) and able for performance in a wide range of temperatures. Already well-established chemical and physical methods of activation allow producing materials with a developed surface area and controlled distribution of pores that determine the electrode / electrolyte interface for electrochemical applications. The possibility of using the activated carbon without binding substance, e.g., fibrous fabrics or felts, gives an additional profit from construction point of view.

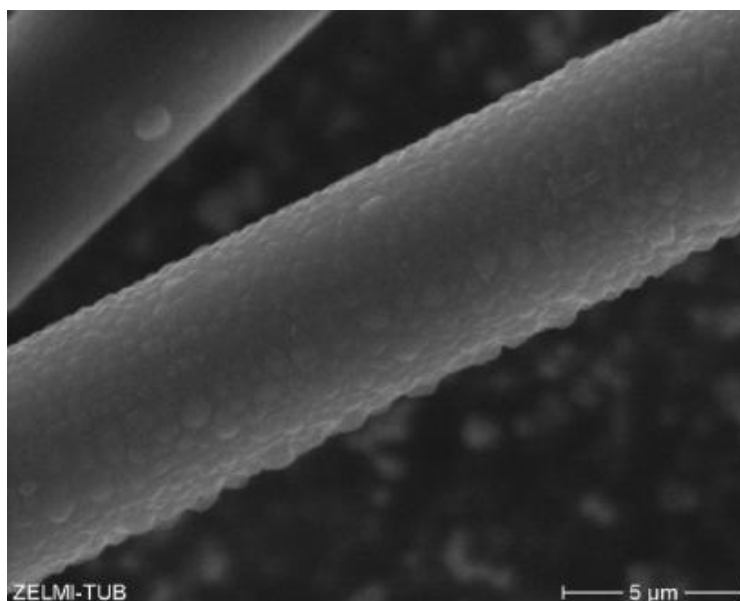


Figure 1.8: SEM image of conductive polymer coated SCFME

Polyacrylonitrile (PAN) type carbon fiber, produced by carbonization of PAN precursor, having high tensile strength and high elastic modulus, extensively applied for structural material composites in aerospace and industrial field and sporting/recreational goods. PAN based fibers are produced from a solubilized mixture that is wet or dry spun to produce a fiber for use in the textile industry. This fiber is stabilized and carbonized to produce a carbon fiber. Aerospace grade material can be obtained in tows that contain between 3000 and 12000 fibers. Lower performance materials are usually formed using larger tows that contain up to 320 000 fibers. PAN based carbon fibers are cheaper when produced from larger tows.

Pitch type of the fiber, produced by carbonization of oil/coal pitch precursor, having extensive properties from low elastic modulus to ultra high elastic modulus. Fibers with ultra high elastic modulus are extensively adopted in high stiffness components and various uses as utilizing high thermal conductivity and / or electric conductivity.

Pitch fibers are melt spun products obtained in small tow sizes varying from 2000 to 4000 fibers. They are larger diameter (10-15 μm) than fibers formed from PAN. The most important mechanical and physical properties exhibited by carbon fibers are the elastic modulus, tensile strength, electrical and thermal conductivities. Carbon fibers are used in fiber-reinforced composites, which consist of fiber and resin. Original large-scale applications were in the reinforcement of polymers.

As the technology of textile reinforced composites expanded, a growing demand from the aerospace industry for composite materials with superior properties emerged. In particular, materials with higher specific strength, higher specific modulus and low density were required. Other desirable properties were good fatigue resistance and dimensional stability. Although carbon fibers meet these demands, it is necessary to improve interfacial properties between reinforcing (carbon) fibers and the polymeric matrix.

1.4 Electrochemical Impedance Spectroscopy (EIS)

Electrical resistance is the ability of a circuit element to resist the flow of electrical current. With impedance data a complete description of an electrochemical system is possible. Representations of the electrified interface have gradually evolved from repeated modifications of the model first proposed by Helmholtz [80-81]. Ohm's law (Equ.1.2) defines resistance in terms of the ratio between voltage E and current I .

$$R = \frac{E}{I} \quad (1.2)$$

While this a well known relationship, its use is limited to only one circuit element, the ideal resistor. An ideal resistor has several simplifying properties:

- It follows Ohm's Law at all current and voltage levels.
- It's resistance value is independent of frequency.
- AC current and voltage signals through a resistor are in phase with each other.

The real world contains circuit elements that exhibit much more complex behavior. These elements force us to abandon the simple concept of resistance. In its place impedance is used, which is a more general circuit parameter. Like resistance, impedance is a measure of ability of a circuit to resist the flow of electrical current. Unlike resistance, impedance is not limited by the simplifying properties listed above. Electrochemical impedance is usually measured by applying an AC potential to an electrochemical cell and measuring the current through the cell. We apply a sinusoidal potential excitation frequency and its harmonics. This current signal can be analyzed as a sum of sinusoidal functions.

Electrochemical Impedance is normally measured using a small excitation signal. This is done so that the cell's response is pseudo-linear. In a linear (or pseudo-linear) system, the current response to a sinusoidal potential will be a sinusoidal at the same frequency but shifted in phase.

Impedance is a totally complex resistance encountered when a current flows through a circuit made of resistors, capacitors, or inductors, or any combination of these. Depending on how the electronic components are configured, both the magnitude and the phase shift of an AC can be determined. Because an inductive effect is not usually encountered in electrochemistry, we consider only the simple equivalent circuit, in which no inductor is present.

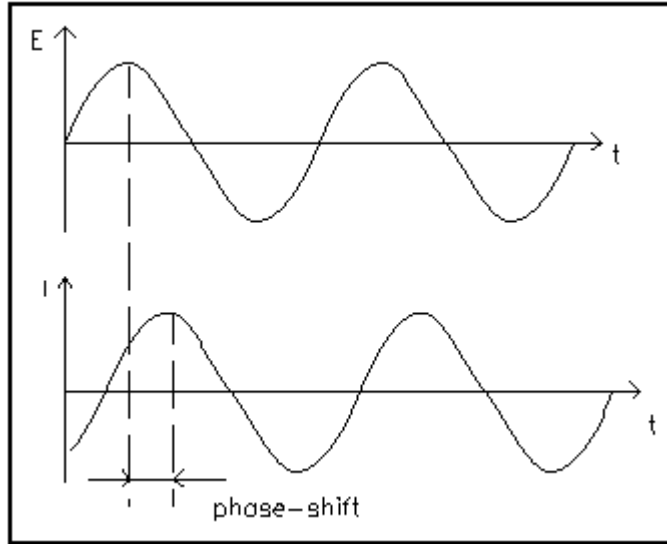


Figure 1.9: Sinusoidal current response in a linear system

The excitation signal, expressed as a function of time, has the form

$$E(t) = E_o \cos(\omega t) \quad (1.3)$$

$E(t)$ is the potential at time t , E_o is the amplitude of the signal, and ω is the radial frequency. The relationship between radial frequency ω (expressed in radians/second) and frequency f (expressed in hertz) is:

$$\omega = 2 \pi f \quad (1.4)$$

In a linear system, the response signal, I_t , is shifted in phase and has a different amplitude, I_o :

$$I(t) = I_o \cos(\omega t - \phi) \quad (1.5)$$

An expression analogous to Ohm's Law allows us to calculate the impedance of the system as:

$$Z = \frac{E(t)}{I(t)} = \frac{E_o \cos(\omega t)}{I_o \cos(\omega t - \phi)} = Z_o \frac{\cos(\omega t)}{\cos(\omega t - \phi)} \quad (1.6)$$

The impedance is therefore expressed in terms of a magnitude, Z_o , and phase shift, ϕ .

By using euler equation;

$$\exp(j\phi) = \cos\phi + j \sin\phi \quad (1.7)$$

It is possible to express the impedance as a complex function. The potential is described as,

$$E(t) = E_o \exp(j\omega t) \quad (1.8)$$

And the current response as,

$$I(t) = I_o \exp(j\omega t - j\phi) \quad (1.9)$$

The impedance is then presented as a complex number,

$$Z = \frac{E}{I} = Z_o \exp(j\phi) = Z_o(\cos\phi + j \sin\phi) \quad (1.10)$$

The expression for $Z(\omega)$ is composed of a real and an imaginary part. If the real part is plotted on the Z axis and the imaginary part on the Y axis of a chart, we get a “Nyquist plot”. Notice that in this plot the Y -axis is negative and the each point on the Nyquist plot is the impedance at one frequency.

By treating the impedance data in such a frequency range, system characteristics for an electrochemical reaction (i.e., R_s , R_p and C_d) can be obtained. R_p is a function of potential; however, at $\eta = 0$, it becomes the charge-transfer resistance R_{CT} . Two convenient ways of treating the impedance data are the Nyquist plot, in which imaginary numbers $Z''(\omega)$ are plotted against real numbers $Z'(\omega)$, and the Bode plot, in which absolute values of impedance or phase angle are plotted against the frequency. Extraction of the system characteristics requires interpreting the Nyquist plot. At high frequencies, $Z(\omega) = Z'(\omega) = R_s$, which is an intercept on the $Z'(\omega)$ axis on the high frequency side ($\phi = 0$ or $Z'' = 0$). For $\omega \rightarrow 0$, it becomes $Z(\omega)$ axis on the low frequency side.

At the frequency where a maximum $Z''(\omega)$ is observed, the straightforward relationship which is the time constant of the electrochemical reaction, can be shown and indicates how fast the reaction takes place. Also, if $R_p \rightarrow C_{dl}$ is known, C_{dl} can be obtained because R_p is already known from the low-frequency intercept on the $Z'(\omega)$ axis.

$$R_p C_{dl} = 1/\omega_{\max} = 1/(2\pi f_{\max}) = \tau_{\text{rxn}} \quad (1.11)$$

The Nyquist plot gives all necessary information about the electrode-electrolyte interface and the reaction. Similar information is obtained by examining the Bode diagram. $\log R_s$ and $\log (R_p + R_s)$ are obtained straightforwardly from the $Z(\omega)$ versus $\log \omega$ plot at high and low frequencies from the same argument as the Nyquist plot. In the intermediate frequency region, an almost straight line with a slope of ~ -1.0 can be seen. On the other hand, contribution and the effect of the Warburg impedance can be important at low frequencies because the mass transport of the electroactive species may limit the electron transfer process.

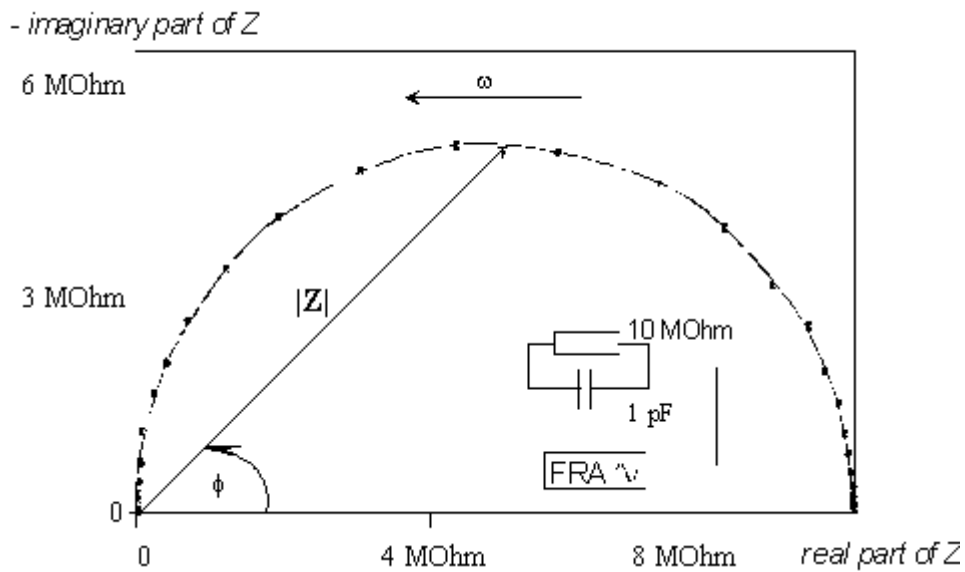


Figure 1.10: Nyquist plot with impedance vector

Nyquist plot has been annotated to show that low frequency data are on the right side of the plot and higher frequencies are on the left. This is true for EIS data where impedance usually falls as frequency rises (this is not true of all circuits). On the Nyquist plot the impedance can be represented as a vector of length Z . The angle between this vector and the x-axis is ϕ .

Nyquist plot have one major shortcoming. The semicircle is characteristics of a single time constant. Electrochemical Impedance plots often contain several time constants. Often only a portion of one or more of their semicircles is seen. Another popular presentation method is the “Bode plot”. The impedance is plotted with log frequency on the x-axis and both the absolute value of the impedance ($Z = Z_o$) and phase-shift on the y-axis. Unlike the Nyquist plot, the Bode plot explicitly shows frequency information.

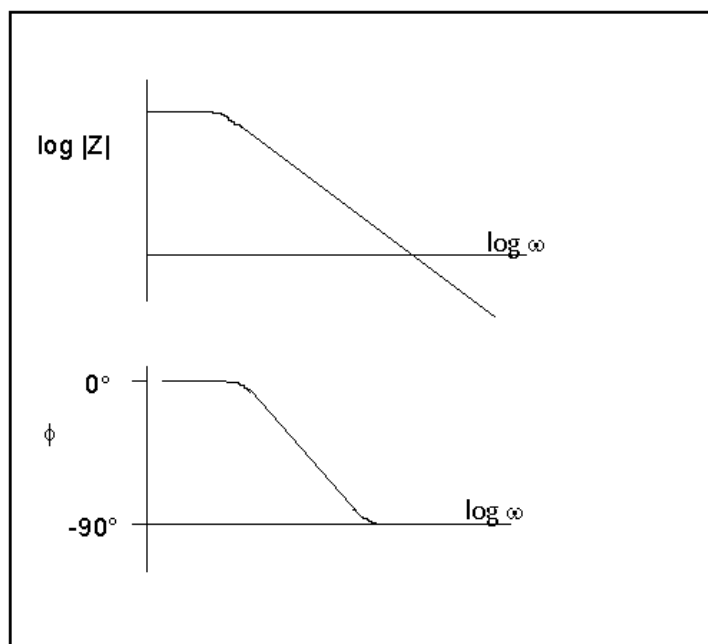


Figure 1.11: Bode plot with one time constant

Impedance of a resistor is independent of frequency and has only a real component. Because there is no imaginary impedance, the current through a resistor is always in phase with voltage. The impedance of an inductor increases as frequency increases. Inductors have only an imaginary impedance component. As a result, an inductor's current in phase shifted 90 degrees with respect to the voltage.

The impedance versus frequency behavior of a capacitor is opposite to that of an inductor. A capacitor's impedance decreases as the frequency is raised. Capacitors also have only an imaginary impedance component. The current through a capacitor is phase shifted-90 degrees with respect to voltage.

Table 1.1: Common electrical elements

Component	Current Vs. Voltage	Impedance
Resistor	$E = IR$	$Z = R$
Inductor	$E = L \, di/dt$	$Z = j\omega L$
Capacitor	$I = C \, dE/dt$	$Z = 1/j\omega C$

1.4.1 Equivalent circuit elements

Equivalent circuit models employ mathematical or computer models of fundamental electric circuit components, such as resistors and capacitors, to model complex electrochemical processes. Simple equivalent circuits have long been used to predict the performance characteristics of porous electrodes.

These equivalent circuits primarily have been applied to attempt to capture the behavior of the double-layer at the interface between the electrode pores and electrolyte solution.

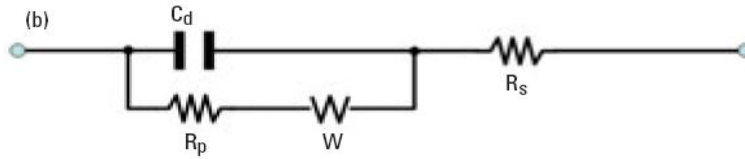


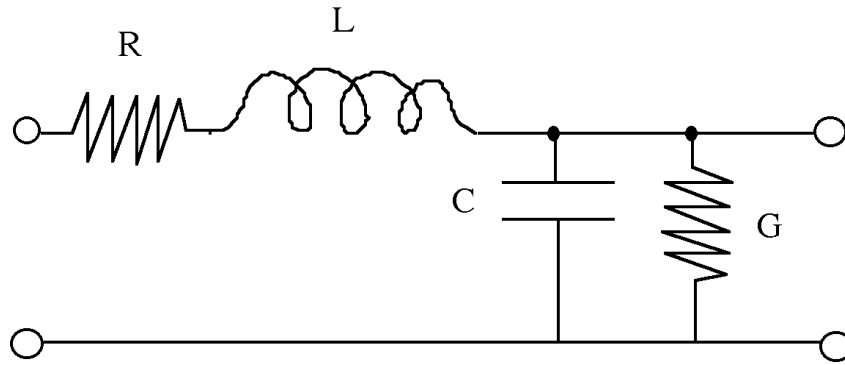
Figure 1.12: An equivalent circuit representing each component at the interface and in the solution during an electrochemical reaction is shown for comparison with the physical components. C_{dl} , double layer capacitor; R_p , polarization resistor; W , Warburg resistor ; R_s , solution resistor

Note that, circuits could be used to model a pseudocapacitor model proposes that, because of unique electrosorption behavior found in micropores, the capacitance per micropore surface area and capacitance per external surface area must be calculated separately. The second model, which is now widely accepted, suggests that electrolyte ions cannot diffuse into pores beneath a size threshold and therefore the surface area of those pores cannot contribute to the capacitance. In considering the second model, there have been efforts to determine the optimal pore size and size distribution needed to maximize ion accessibility. As a corollary result, an inverse relationship between pore size and ESR has also been demonstrated.

Table 1.2: Circuit elements used in the models

Equivalent element	Admittance	Impedance
R	$1/R$	$j\omega C$
C	$j\omega C$	$1/j\omega C$
L	$1/j\omega L$	$j\omega L$
W(Infinite)	$Y_o\sqrt{(j\omega)}$	$1/Y_o\sqrt{(j\omega)}$
O (Finite)	$Y_o\sqrt{(j\omega)} \coth(B\sqrt{(j\omega)})$	$Tanh(B\sqrt{(j\omega)})/Y_o\sqrt{(j\omega)}$
Q(CPE)	$Y_o(j\omega)\alpha$	$1/Y_o(j\omega)\alpha$

Looking at the electrode/polymer/electrolyte system from the viewpoint of the impedance characteristics, at variance with an electrified membrane inside an electrolytic solution, it constitutes a so-called ‘asymmetrical’ configuration [82], the current flow requiring the transport of electrons across the metal/polymer interface and of ions through the polymer/electrolyte interface; the charge percolation inside the polymer bulk should be additionally considered.

**Figure 1.13:** Transmission line circuit model.

The generalised transmission line circuit model predicts the relevant impedance features of such a system in terms of a Nyquist plot, based on a mathematical approach. The two semi-circles at the highest frequencies, induced by the processes at the metal/polymer and polymer/solution interfaces, are, in practice, not always detectable. Sometimes, only one or even one-half semi-circle is observed; at other times, these two semi-circles are partially overlapped to each other, the actual situation observed depending on the characteristics of the interfacial processes in terms of energy (resistance) to overcome at the relevant interface.

Moreover these semi-circles are very often depressed, most probably due to non-homogeneous separation surfaces [83]. Furthermore, they can also overlap to the mid-frequency Warburg impedance quasi-45°-slope segment that reflects the diffusion-migration of ions at the boundary surface between solution and polymer, inside the latter medium. Finally, 90°-trend at the lowest frequencies, due to a capacitive impedance, accounts for the charge transport process inside the bulk of the film.

An ionic conductivity often constitutes the slow step in the overall charge percolation process through the CP-modified electrode system [84]. When the ionic conductivity is definitely very low, so that a very thin diffusion layer accounts for the transport of ions inside the polymer, the generalised transmission line-circuit can be considered infinitely extended, simulating a semi-infinite diffusion-migration, the boundary surface being the polymer/solution one.

Therefore, the trend attributable to a Warburg impedance extends so much down to low frequencies that the capacitive impedance 90°-slope trend may not be observed. In this case the generalised transmission line circuit can be simplified into the classical Randles circuit.

On the opposite side, when the ionic conductivity is relatively high, the impedance value of the polymer bulk is correspondingly low, both ions being present in the bulk of the permselective polymer. The study of this situation for the case of polypyrrole, carried out by Duffit and Pickup [85-86], has led the authors to define a condition they call 'enhanced ionic conductivity': for polypyrrole, electrolyte concentrations as high as 3 M are proposed.

For intermediate situations the whole generalised transmission line circuit has to be considered. In the impedance plot of such a circuit the presence of an additional semi-circle at the highest frequencies is also predictable, which is described to the impedance of the polymer bulk but cannot, however, be generally observed using instrumentation with non-extraordinary performances. If one is mainly interested in the study of ionic conductivity, the generalised transmission line circuit can then be simplified into the circuit proposed by Albery and Mount [87].

1.4.1.1 Electrolyte resistance

Solution resistance is often a significant factor in the impedance of an electrochemical cell. A modern three electrode potentiostat compensates for the solution resistance between the counter and reference electrodes.

The resistance of an ionic solution depends on the ionic concentrations, type of ions, temperature and the geometry of the area in which current is carried. In a bounded area with area A and length l carrying a uniform current the resistance is defined as:

$$R = \rho \cdot l/A \quad (1.12)$$

In this equation R is the solution resistivity. The conductivity of the solution, k , is more commonly used in solution resistance calculations. Its relationship with solution resistance is:

$$R = l/k.A \text{ as a result } k = l/R.A \quad (1.13)$$

For other solutions, k was calculated from specific ion conductance. The units for k are Siemens per meter (S/m). The siemens is the reciprocal of the ohm, so $S = 1/\text{Ohm}$. The value of the double layer capacitance depends on many variables including electrode potential, temperature, ionic concentrations, types of anions, oxide layers, electrode roughness, impurity adsorption, etc.

1.4.1.2 Double layer capacitance (C_{dl})

An electric double layer exists at the interface between an electrode and its surrounding electrolyte. This double layer is formed as ions from the solution stick on the electrode surface. Charges in the electrode are separated from the charges of these ions. The separation is very small, on the order of angstroms.

1.4.1.3 Polarization resistance

Whenever the potential of electrode is forced away from its value at open circuit, is referred to as polarizing the electrode. When an electrode is polarized, it can cause current to flow via electrochemical reactions that occur at the electrode surface. The amount of current is controlled by the kinetics of the reactions and the diffusion of reactants both towards and away from the electrode.

In cells where an electrode undergoes uniform corrosion at open circuit, the open circuit potential is controlled by the equilibrium between two different electrochemical reactions. One of the reactions generates cathodic current and the other anodic current. The open circuit potential ends up at the potential where the cathodic and anodic currents are equal each others. It is referred to as a mixed potential. The value of the current for either of the reactions is known as the corrosion current, a new parameter, R_p , the polarization resistance.

1.4.1.4 Diffusion

Diffusion can create impedance known as the Warburg impedance. This impedance depends on the frequency of the potential perturbation. At high frequencies the Warburg impedances small since diffusing reactants don't have to move very far. At low frequencies the reactants have to diffuse further, thereby increasing the Warburg impedance. The equation for the infinite Warburg impedance is:

$$Z = \sigma (\omega)^{-1/2} (1-j) \quad (1.14)$$

On a Nyquist plot the infinite Warburg impedance appears as a diagonal line with a slope of 0.5. On a Bode plot, the Warburg impedance exhibits a phase shift of 45° .

1.4.1.5 Constant phase element

Capacitors in EIS experiments often do not behave ideally. Instead, they act like a constant phase element (CPE) as defined below. The impedance of a capacitor has the form:

$$Z = A(j\omega)^{-a} \quad (1.15)$$

When this equation describes a capacitor, the constant $A=1/C$ (the inverse of the capacitance) and the exponent $a=1$. For a constant phase element, the exponent a is less than one. The double layer capacitor on real cells often behaves like a CPE instead of resembling a capacitor. Several theories have been proposed to account for the non-ideal behavior of the double layer but none has been universally accepted.

1.5 Characterizations

1.5.1 Attenuated total reflection Fourier transform infrared spectroscopy (FTIR-ATR)

Attenuated Total Reflectance (ATR) spectroscopy, known as internal reflection spectroscopy or multiple internal reflectance (MIR), is a versatile, nondestructive technique for obtaining the infrared spectrum of materials either too thick or too strongly absorbing to be analyzed by standard transmission spectroscopy.

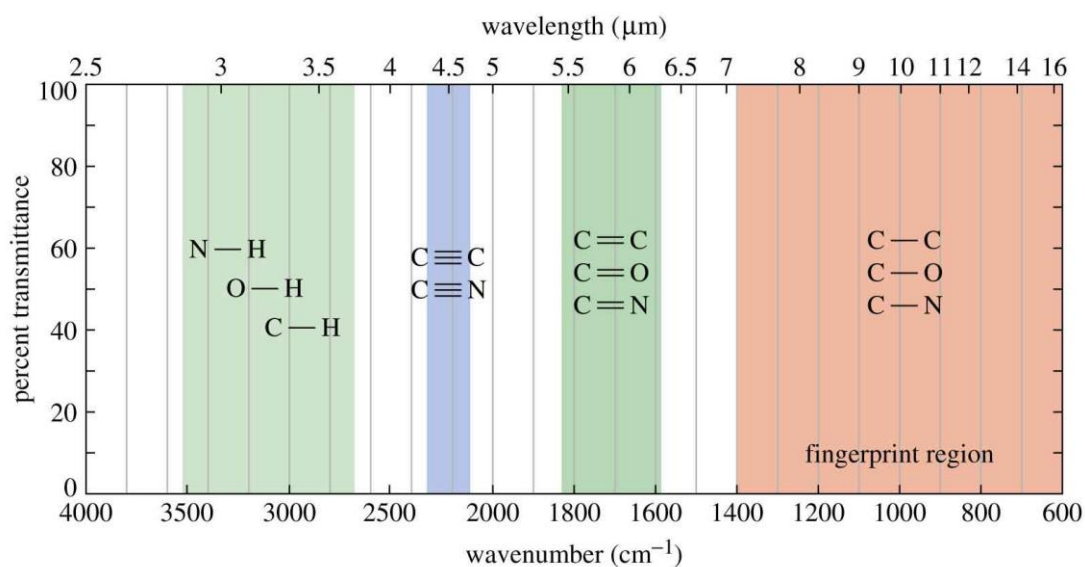


Figure 1.14: Infrared spectrum bands for general substitutions

Attenuated Total Reflectance (ATR) FTIR is widely used by researchers to examine a variety of sample types including solids, powders, pastes and liquids for food analysis, biomedical applications, polymers, and thin films. In addition to the identification of functional groups during more routine analysis, FTIR-ATR spectroscopy is useful for mechanistic studies of vapor-solid interactions during chemical vapor deposition or heterogeneous catalysis by in situ real time monitoring of surface species.

1.5.2 Spectroelectrochemistry

Basic of UV Light Absorption, Ultraviolet / visible spectroscopy involves the adsorption of ultraviolet / visible light by a molecule causing the promotion of an electron from a ground electronic state to an excited electronic state.

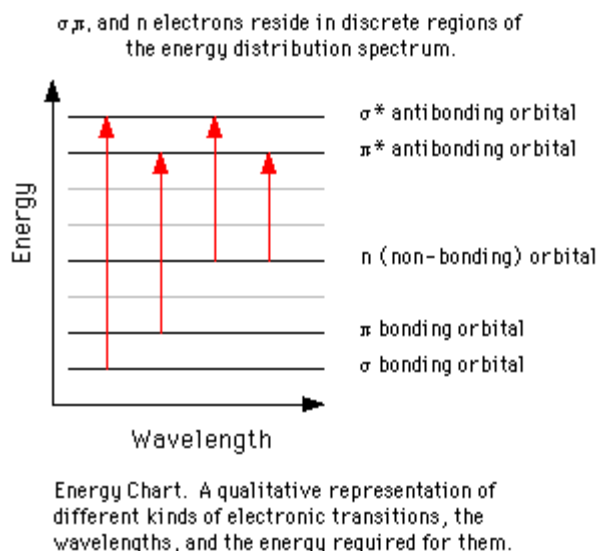


Figure 1.15: Electronic transitions

Transitions from the highest occupied molecular orbital (HOMO) to the lowest occupied molecular orbital (LUMO) require the least amount of energy and are therefore usually the most important. Not all transitions that are possible will be observed. Some electronic transitions are forbidden by certain selection rules. However, even forbidden transitions can be observed, but these are usually not very intense. Peak Broadening UV absorptions are generally broad because vibrational and rotational levels are superimposed on top of the electronic levels.

1.5.3 Scanning electron microscopy (SEM)

Scanning electron microscope (SEM) is a type of electron microscope capable of producing high resolution images of a sample surface. SEM images have a characteristic three-dimensional appearance and are useful for judging the surface structure of the sample.

In a typical SEM electrons are thermionically emitted from a tungsten or lanthanum hexaboride (LaB_6) cathode and are accelerated towards an anode; alternatively electrons can be emitted via field emission (FE). Tungsten is used because it has the highest melting point and lowest vapour pressure of all metals, thereby allowing it to be heated for electron emission.

The electron beam, which typically has an energy ranging from a few hundred eV to 50 keV, is focused by one or two condenser lenses into a beam with a very fine focal spot sized 1 nm to 5 nm. The beam passes through pairs of scanning coils in the objective lens, which deflect the beam in a raster fashion over a rectangular area of the sample surface. Through these scattering events, the primary electron beam effectively spreads and fills to teardrop-shaped volume, known as the interaction volume, extending from less than 100 nm to around 5 μm into the surface. Interactions in this region lead to the subsequent emission of electrons which are then detected to produce an image. X-rays, which are also produced by the interaction of electrons with the sample, may also be detected in an SEM equipped for energy-dispersive X-ray spectroscopy or wavelength dispersive X-ray spectroscopy.

The nature of the SEM's probe, energetic electrons, makes it uniquely suited to examining the optical and electronic properties of semi-conductor materials. The high-energy electrons from the SEM beam will inject charge carriers into the semi-conductor. Thus, beam electrons lose energy by promoting electrons from the valence band into the conduction band, leaving behind holes.

In direct bandgap material, recombination of these electron-hole pairs will result in cathodoluminescence; if the sample contains an internal electric field, such as is present at a p-n junction, the SEM beam injection of carriers will cause electron beam induced current (EBIC) to flow.

1.5.4 Atomic force microscopy (AFM)

For qualitative analysis in fractography, SEM (scanning electron microscopy) and stereoscopic techniques are widely used but are limited by quantitative measurements on the surface such as, roughness and striations on fractured surface. Therefore, the implementation of a reliable and specialized qualitative and quantitative technique that can reveal the three-dimensional characteristics of the surface and the study of the related parameters is necessary. At the microscopic and submicroscopic scales such possibility is now offered by atomic force microscopy (AFM).

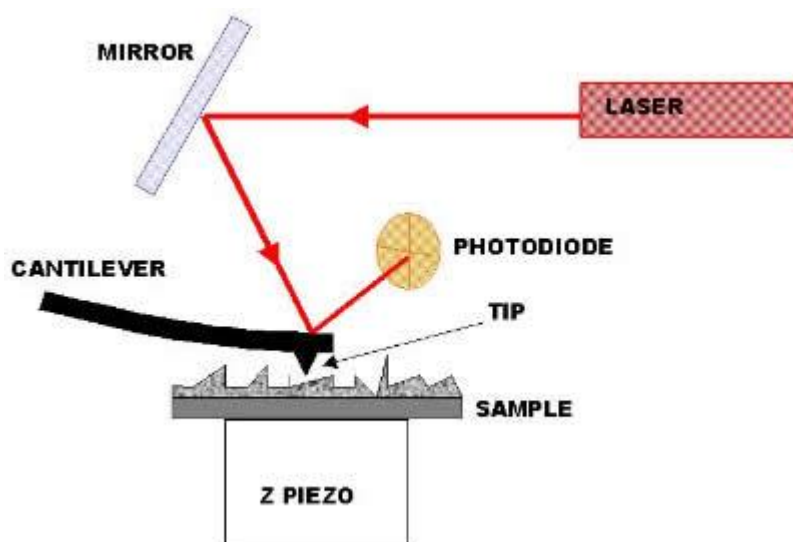


Figure 1.16: Schematic diagram of atomic force microscope

Figure 1.15 shows the AFM scheme, which consists of a cantilever and an integrated tip as shown in Figure 1.17. While the tip makes contact with the sample surface, a laser beam focused on the back of the cantilever, reflects onto a quadrant photo detector. The deflection in cantilever due to applied normal and lateral forces can be measured by monitoring the variation in the photodetector signal. This allows the force detection in the nano-Newton to pico-Newton (10^{-9} to 10^{-12} N) regime.

The principles of operation of an AFM are very simple: an extremely, usually atomically, sharp tip made of Si or Si_3N_4 is micro machined at the end of a flexible cantilever. The sensors used in this study were of silicon. It is then positioned in close proximity of the sample surface, where the cantilever is bent by the atomic force between the tip and sample surface. This tip is a contact-mode nano-sensor, with a tip radius of 7 – 10 nm and 30 nm aluminum reflex coating on cantilever side that improves reflectivity.

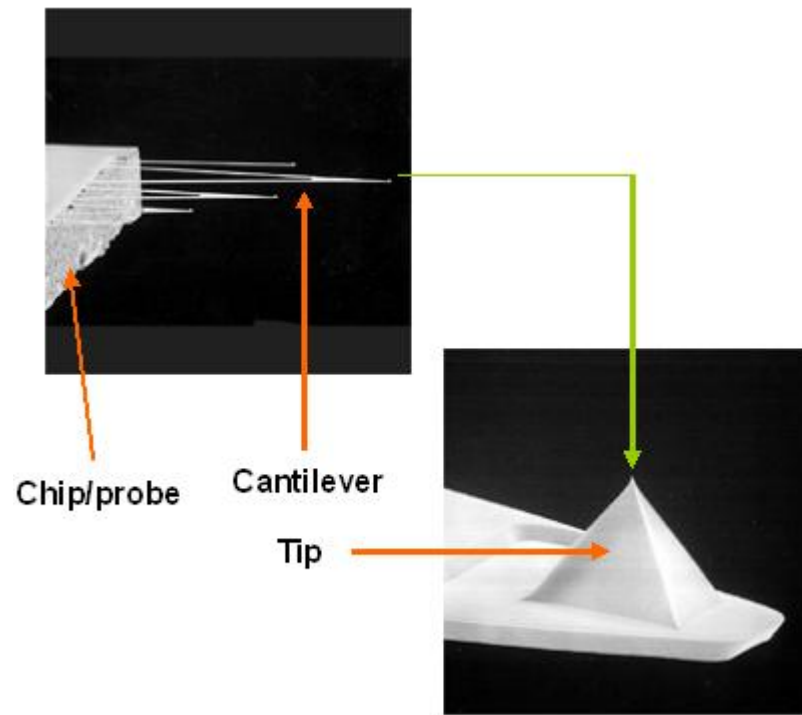


Figure 1.17: Schematic AFM contact mode probe

The AFM is most often compared with the electron beam techniques such as the SEM or TEM. In general, it is easier to learn to use AFM than SEM because there is minimal sample preparation required with an AFM. With an AFM, if the probe is good, a good image is measured.

2. EXPERIMENTAL

2.1 Chemicals

3,4-Ethylenedioxythiophene (EDOT) monomer (obtained from Sigma-Aldrich) and N-phenylsulfonyl pyrrole (PSP) monomer (supplied by Aldrich Chem. Co) were used in the study. Electrochemical polymerizations (electrocoatings) were performed in acetonitrile (ACN, LiChrosolv Reag., Merck) containing NaClO₄ (Sigma) with a same scan rate of 30mV/s, and a deposition cycle of 10 (applied charges).

2.2 Electrocopolymerizations

Electrocopolymerizations by cyclic voltammetry were performed using a Princeton Research Potentiostat (model 2263) potentiostat/galvanostat, interfaced to a PC computer with Power Suite Software package. The potentiostat was also connected to a Faraday cage (BAS Cell Stand C3). A three electrode system, employing carbon fiber as working electrode, Pt button as counter electrode and Ag button as a reference electrode, was used.

2.3 Electrode Preparations

SGL SIGRAFIL C 320B (A carbon fiber with high strength, high modulus of elasticity, and high electric conductivity, manufactured by SGL Carbon Group) containing single filaments in a roving was used as the working electrode. Fabrication of all single carbon fiber micro electrodes (SCFMEs) was carried out as follows.

A single carbon fiber SGL SIGRAFIL HM485 (~ 7μm in diameter, approx. 4 cm in length) was inserted onto a 5 cm long teflon tape, while 2.5 cm of the fiber was kept out. A filament of carbon fibers with a length of 8 cm (approximately 25 fibers) were stucked onto the single carbon fiber for providing connections and electrical conductivity. A second teflon tape with the same length was mounted and wrapped

around the composition. Silver paste was used on carbon fiber filament to improve conductivity.

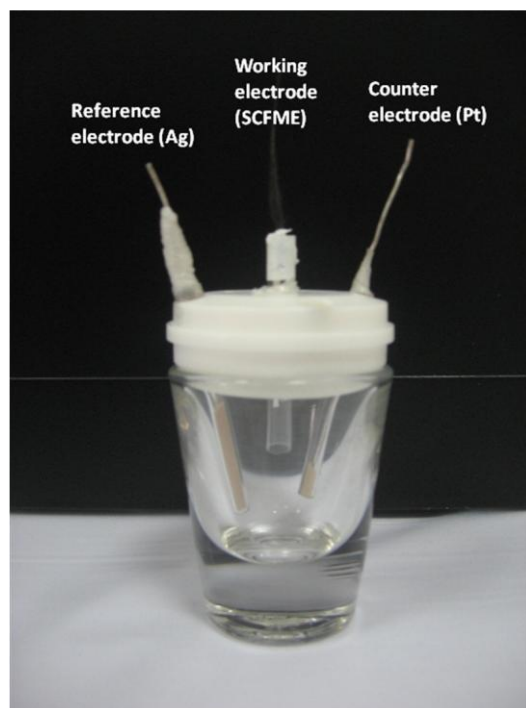


Figure 2.1: A geometry of one compartment-3 electrode cell

A multimeter was used to test the conductivity. Then SCFME, initially cleaned in acetone for 2 minutes and rinsed with distilled water, was dried at room temperature. The electrode area was kept constant $\sim 2 \times 10^{-3} \text{ cm}^2$ by adjusting the dipping length ($\sim 1 \text{ cm}$). The button electrodes were prepared by using Ag and Pt wires in glass pipes ($\sim 4.45 \text{ mm}$ diameter) filled with methylmetacrylate (MMA), electrodes were then polymerized by UV light, which was inert against the electrolyte solution. The surface area of the reference and the counter electrodes were kept constant ($\sim 0.47 \text{ mm}^2$) during the experiments.

2.4 Electrochemical Impedance Spectroscopy (EIS) and Equivalent Circuit Modelling (ECM)

EIS measurements were taken at room temperature ($\sim 25^\circ \text{C}$) using a conventional three electrode cell configuration. The electrochemical cell was connected to a Potentiostat (PAR 2263) connected to a PC. An electrochemical impedance software, PowerSine, was used to carry out impedance measurements between 10 mHz and

100 kHz, with an applied AC signal amplitude of 10mV. The impedance spectra was analyzed using ZSimpWin V3.10, an AC-impedance data analysis software.

2.5 Fourier Transform Infrared-Attenuated Total Reflectance (FTIR-ATR)

For spectroscopic measurements, Poly(EDOT-co-PSP) copolymers were synthesized at a constant potential (0.8 V), using Steel plates with different monomer concentration ratios in a NaClO₄/ACN solution. Polymer films on the steel plate were then removed and analysed using an ATR-FTIR reflectance spectrometer (Perkin Elmer, Spectrum One; having a universal ATR attachment with a diamond and ZnSe crystal C70951). Perkin Elmer Spectrum software was used to carry out FTIR-ATR measurements between 650-4000 cm⁻¹.

2.6 Ultra-Violet/Visible Spectrophotometric Measurements (UV/Vis)

Oligomers of copolymers were dissolved in electrolyte solution during electropolymerization, resulting in colored solutions, measured by a Perkin Elmer Lambda 45 UV/Vis Spectrometer. Perkin Elmer UV Winlab software was used to carry out UV/Vis measurements between 300-800 nm.

2.7 Scanning Electron Microscopy (SEM)

Thin films of copolymers, electrocoated onto carbon fibers were analyzed by scanning electron microscopy on a Nanoaye Desktop Mini-SEM Instrument. The excitation energy used 5 keV. Average values of the increase in fiber thickness were obtained from SEM images, taking into account the diameter of the ungrafted fiber. The diameters for the fibers were calculated from an average of 5-6 measurements on individual fibers.

2.8 Atomic Force Microscopy (AFM)

Thin film of copolymers, electrocoated onto silicon wafer, were analyzed by atomic force microscopy using a Nanosurf Easyscan AFM Instrument with a 10 μm AFM head. The Nanosurf Easyscan 2 software was used to carry out the AFM measurements.

3. RESULTS AND DISCUSSIONS

3.1 The Experimental Details of Electrochemical Copolymerization of 3,4-Ethylenedioxythiophene (EDOT) and N-Phenylsulfonyl Pyrrole (PSP) on SCFME in Different Mole Fractions of PSP

The oxidation potential of a chemical system is a measure of tendency for oxidation reactions to occur in that system [88]. Each of elements or ions has its own characteristic oxidation potential, that is, has a characteristic tendency to oxidize, as dictated by binding energy of the electrons in the atom and the energy of the solvation of ions [89].

Synthesis of polymer films on SCFMEs were performed cyclic voltammetrically at normal ambient conditions on 1 cm long dipped into ~5 ml electrolytic solution, using a standart three electrode cell (surface area of working electrode is $2 \times 10^{-3} \text{ cm}^2$). Pt and Ag button electrodes were used as counter and pseudo reference electrodes, respectively (each was placed ~ 1 cm distance from each other).

For electrocopolymerization of EDOT and PSP, 10 mM PSP and 5, 1.6, 1, 0.5 mM EDOT was used. Electrocopolymerizations were performed for the monomers with 0.1 M NaClO_4 in ACN at a scan rate of 30 mV.s^{-1} and 10 cycles.

After EDOT and PSP were electrochemically polymerized on SCFME, the working electrode (modified SCFME) was removed from the cell and then washed throughly with ACN to remove monomer molecules and electrochemical impedance measurements were carried out in the same electrolyte solution.

Finally, modified carbon fibers were characterized in monomer free solutions to find out their redox behavior at different scan rates between 25 mV.s^{-1} and 200 mV.s^{-1} by cyclic voltammetry.

3.2 Electrocopolymerization of EDOT and PSP

Multisweep cyclic voltammograms of PSP (10 mM) in the presence of EDOT (5.0; 1.6; 1.0; 0.5 mM) at (-0.8 – 1.3) V in 0.1 M NaClO₄/ACN on SCFME show an increase in current density with each cycle ($E_{pa} = 0.1$ V, $E_{pc} = 0.0$ V at 10th cycle), resulting in the formation of a thin film of conducting copolymers on SCFME (at 30mV/s scan rate and 10cycle) Fig. 2.1a-c.

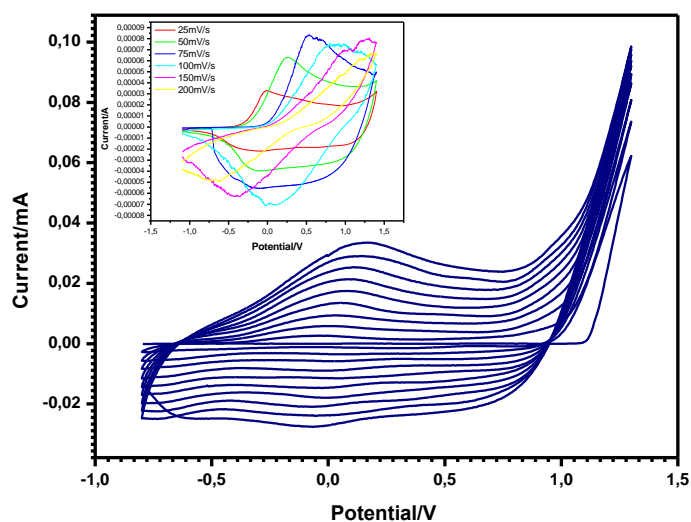


Figure 3.1: Cyclic voltammogram of electrogrowth of 10 mM PSP and 5 mM EDOT in 0.1 M NaClO₄/ACN at 30mV.s⁻¹, 10 cycle on SCFME. Inset: CV of monomer free of Poly(EDOT-co-PSP) film in 0.1 M NaClO₄/ACN different scan rates between 25 and 200 mV.s⁻¹

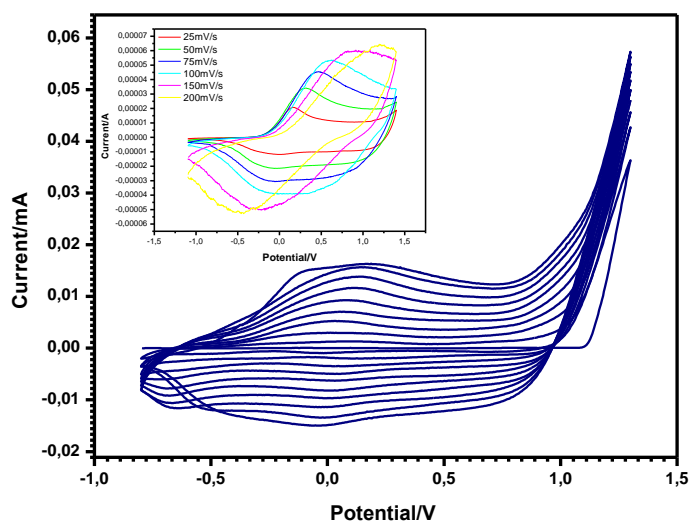


Figure 3.2: Cyclic voltammogram of electrogrowth of 10 mM PSP and 1.66 mM EDOT in 0.1 M NaClO₄/ACN at 30mV.s⁻¹, 10 cycle on SCFME. Inset: CV of monomer free of Poly(EDOT-co-PSP) film in 0.1 M NaClO₄/ACN different scan rates between 25 and 200 mV.s⁻¹

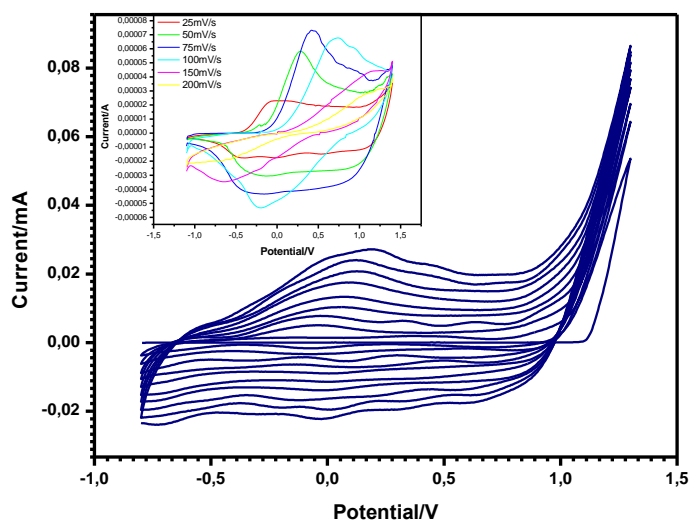


Figure 3.3: Cyclic voltammogram of electrogrowth of 10 mM PSP and 1 mM EDOT in 0.1 M NaClO₄/ACN at 30mV.s⁻¹, 10 cycle on SCFME. Inset: CV of monomer free of Poly(EDOT-co-PSP) film in 0.1 M NaClO₄/ACN different scan rates between 25 and 200 mV.s⁻¹

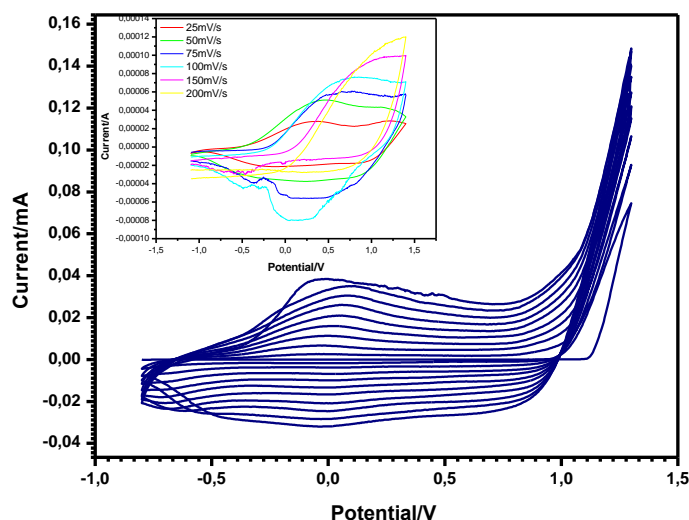


Figure 3.4: Cyclic voltammogram of electrogrowth of 10 mM PSP and 0.5 mM EDOT in 0.1 M NaClO₄/ACN at 30mV.s⁻¹, 10 cycle on SCFME. Inset: CV of monomer free of Poly(EDOT-co-PSP) film in 0.1 M NaClO₄/ACN different scan rates between 25 and 200 mV.s⁻¹

Redox behavior of the resulting copolymers was investigated in the same electrolyte solution by cyclic voltammetry (CV). The inset plots of Figures 3.1-3.4 present cyclic voltammograms of Poly(PSP-co-EDOT)s in monomer-free solutions at different scan rates (25 to 200 mV/s), indicating a regular growth and a linear increase in peak currents (oxidation and reduction peaks). Also these oxidation and reduction peaks have nearly the same value as the corresponding peaks obtained from cyclic voltammetry of electrochemical growth.

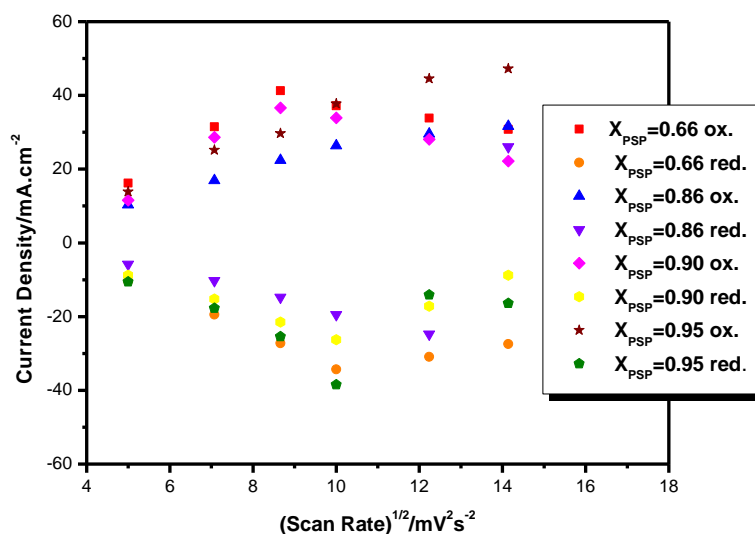


Figure 3.5: Plot of anodic and corresponding cathodic peak current density vs. the scan rate of the Poly(EDOT-co-PSP) films in different electrolyte solutions

The scan rate dependencies of the Poly(EDOT-co-PSP) films are presented in Figure 3.5. Both oxidation and reduction peaks of the copolymer films were plotted using current density values with respect to the scan rate. Square root of scan rates until 10 $\text{mV}^2.\text{s}^{-2}$, show linear plot, that is due to formation of electroactive copolymer and indication of the electroactive copolymer films which are well adhered and redox processes are generally it seems non-diffusion limited.

3.3 Ex-situ FTIR-ATR Measurements of Poly(EDOT-co-PSP) and PEDOT

Inclusion of PSP into the electrocopolymerized thin film, and doping with the respective anion of the supporting electrolyte were followed by FTIR-ATR (Fig. 3.7-3.8). This technique allows us to assign corresponding functional groups in the resulting copolymer. For spectroscopic characterization of Poly(EDOT-co-PSP) films, the same mole fractions of the copolymers were also prepared by chronoamperometry at 0,8V, on steel plates with the same conditions of Poly(EDOT-co-PSP) film formation on SCFME.

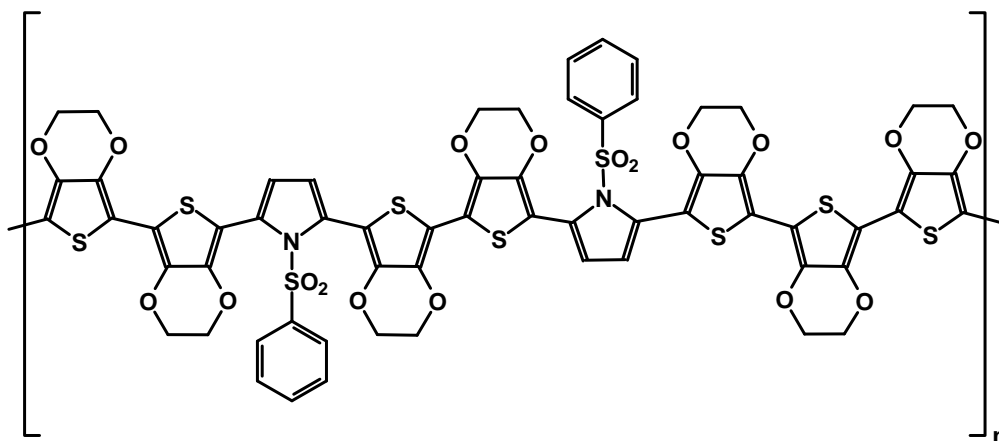


Figure 3.6: Chemical structure of Poly(EDOT-co-PSP)

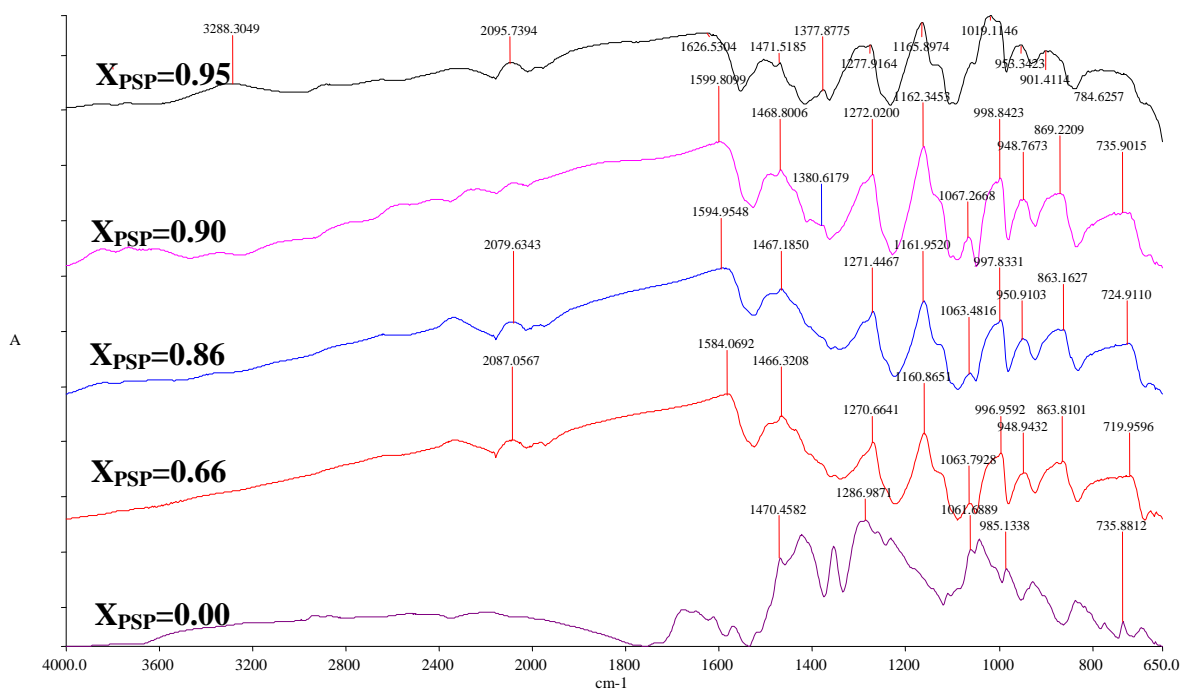


Figure 3.7: Ex-situ FTIR-ATR spectrum of Poly (EDOT-co-PSP) and PEDOT powders obtained via chronoamperometry method on steel plates

The band at 1470 cm⁻¹ (stretching of C=C bond) and the peak at 1227 cm⁻¹ (the stretching quonidal structure of thiophene) are known to be characteristic vibrational peaks of polythiophene. Vibrations at 3228 cm⁻¹ originate from the N-H wagging in the pyrrole ring. The band at 1584-1626 cm⁻¹ is known to be C-H bending and ring puckering peak of the aromatic ring of PSP. Sulfonyl stretching at 1376 cm⁻¹ becomes distinct when PSP ratio is increased in the copolymer. Further vibrations

from the C-S bond, in the thiophene ring, can be seen at 719-784 cm^{-1} , attributed to C-S stretching. Vibrations at 1063 cm^{-1} are assigned to the stretching in the alkylendioxy group.

Table 3.1: FTIR-ATR assignments of Poly(EDOT-co-PSP)s

(cm^{-1})	$X_{\text{PSP}}=0.00$	0.66	0.86	0.90	0.95
N-H wagging	-	-	-	-	3228
C-H deformation (aromatic)	-	2087	2079	-	2095
C-H bend. and ring puckering	-	1584	1594	1599	1626
C=C str.	1471	1466	1467	1468	1471
Sulfonyl str.	-	-	-	1380	1377
The str. quonidal structure of thiophene	1286	1270	1271	1272	1277
C-H in plane bend. (aromatic)	-	1160	1161	1162	1165
C-O-C group str.	1061	1063	1063	1067	1062
C-O bend.	985	996	997	998	1019
C-H bend. (aromatic)	-	948	950	948	953
S-OR str. (esters)	-	863	863	869	901
C-S str.	735	719	724	735	784

In Figure 3.8, the assigned peak areas were obtained from FTIR-ATR spectrums. Vibrations at 948-953 cm^{-1} are known to be C-H bending in phenyl ring of the PSP. By increasing the PSP ratio in the copolymer, the peak areas of PSP increased. This result should be considered an evidence for the participation of PSP in the copolymer structure.

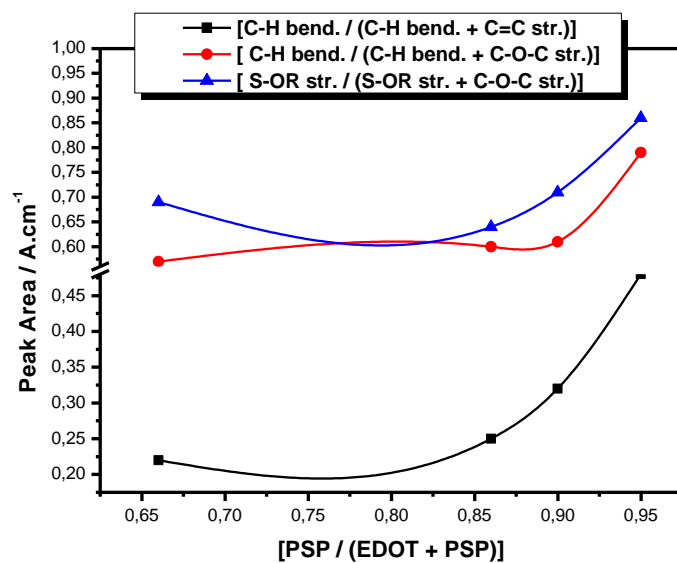


Figure 3.8: Comparison of FTIR-ATR peak area ratios to understand the presence of PSP in copolymer

3.4 Ex-situ UV-Vis Spectrophotometric Measurements of EDOT-PSP and EDOT Oligomers

Oligomers formed in the solution during the electrocopolymerizations of EDOT and PSP at constant potential onto steel plate (for FTIR-ATR characterizations) were followed by UV-Vis spectroscopy.

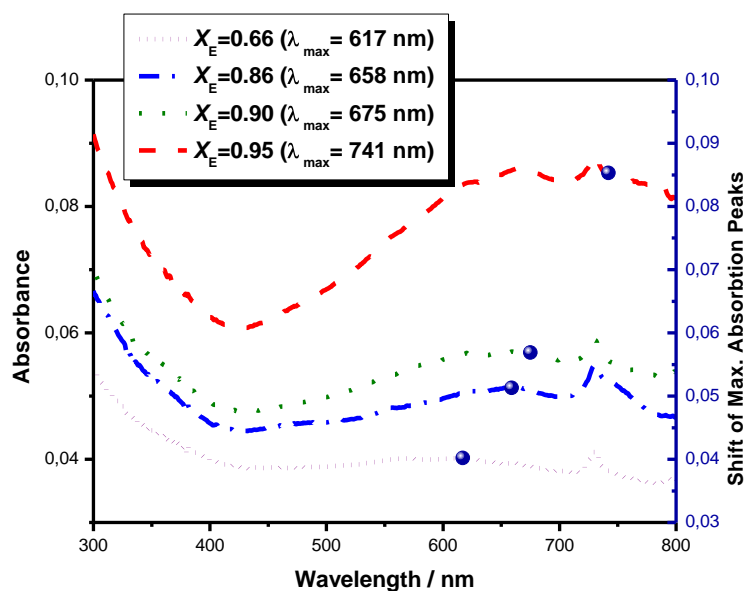


Figure 3.9: Ex-situ spectroelectrochemical measurements (UV-Vis) of different mole fractions of EDOT-PSP oligomers

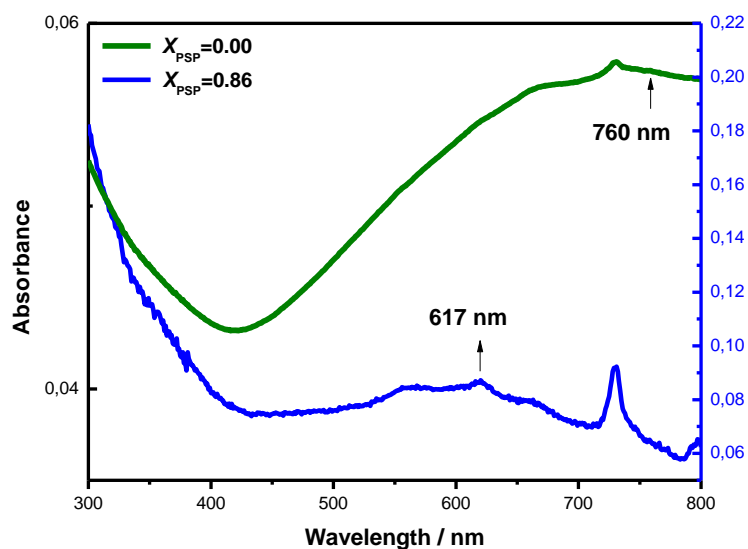


Figure 3.10: Ex-situ spectroelectrochemical measurements (UV-Vis) of EDOT ($X_{\text{PSP}}=0.00$) and EDOT-PSP ($X_{\text{PSP}}=0.86$)

The ex-situ UV-Vis spectra were recorded in ACN for different molar ratios of EDOT-PSP oligomers, exhibiting peaks between 610-740 nm, corresponding to the possible electronic transitions of π , σ and n electrons. (bonding level to the antibonding state of bipolaron, polaron bonding level to the π^* conduction band and valence band to the conduction band, respectively)[90]. PSP did not polymerize under the same conditions onto the steel plate. In Fig. 3.9, it is shown that the absorbance of oligomer peaks (possibly low molecular weight of polymers) increases and the maximum absorption peaks shift while PSP ratio increases in the copolymer. In the UV-Vis spectrum of EDOT oligomer, measured in ACN, only one main absorption peak could be observed at 760 nm (solution color: purple). By the addition of 10 mM PSP, the peak shifted to 620 nm (solution color: blue-black) (Fig. 3.10).

3.5 EIS Investigation and Equivalent Circuit Modelling of Poly(EDOT-co-PSP) on SCFME

Electrochemical Impedance Spectroscopy (EIS) measurements were performed for different monomer concentration ratios of the Poly(PSP-co-EDOT) in monomer-free electrolyte solution, where stability of the film exhibited good electroactivity without undergoing deformation. The low frequency capacitance (C_{LF}) values from the impedance spectroscopy were obtained from the following equation, using imaginary component (Z_{IM}) corresponding to $f = 0.01$ Hz,

$$C_{LF} = -1/2\pi f Z_{IM}$$

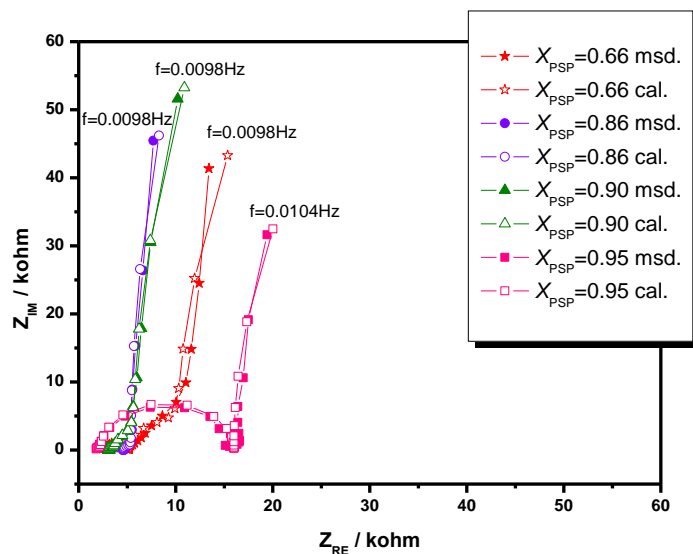


Figure 3.11: Nyquist Plots of Poly(EDOT-co-PSP)s electrografted on SCFMEs correlated with the calculated data from the equivalent circuit modelling; $R(C(R(Q(RW))))$

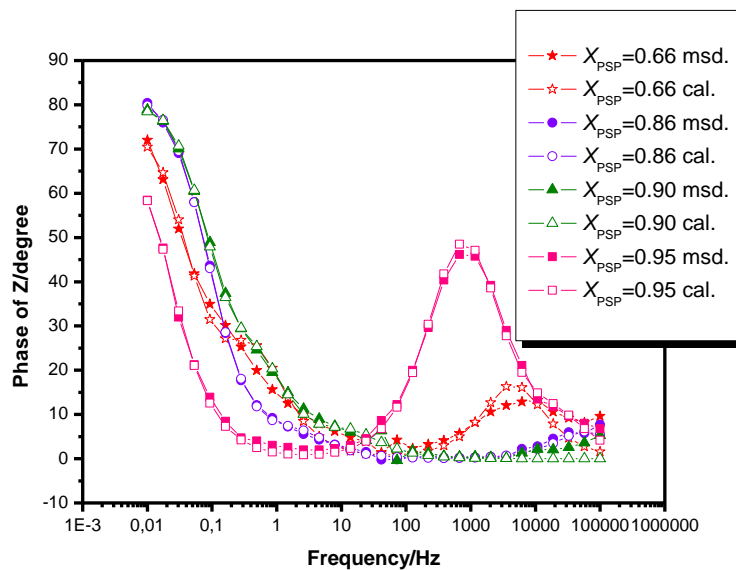


Figure 3.12: Bode Phase Plots of Poly(EDOT-co-PSP)s electrografted on SCFMEs correlated with the calculated data from the equivalent circuit modelling; $R(C(R(Q(RW))))$

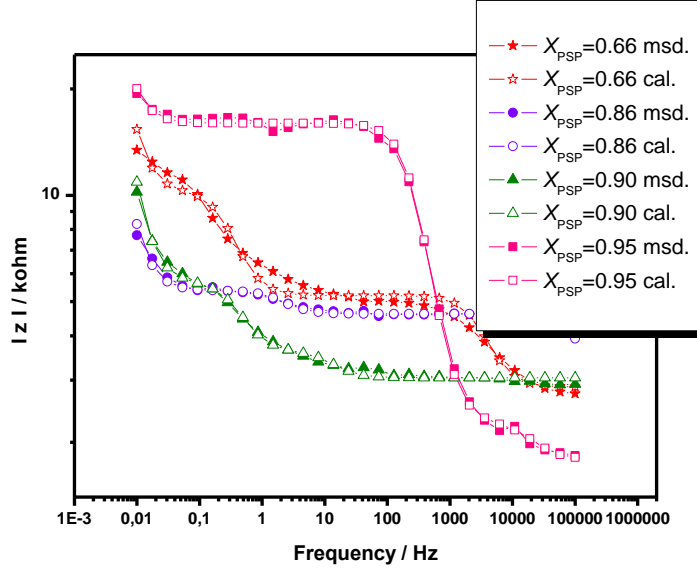


Figure 3.13: Magnitude Plots of Poly(EDOT-co-PSP)s electrografted on SCFMEs correlated with the calculated data from the equivalent circuit modelling; $R(C(R(Q(RW))))$

Figure 2.6(a) illustrates Nyquist plots of the Poly(EDOT-co-PSP) films where the magnitude of the imaginary parts are very large for all mole fractions. The system shows capacitive behaviour for all values. As seen in Table 3.2, the maximum capacitance value at low-frequency (C_{LF}) was obtained for $X_{PSP}=0.86$. Also, $X_{PSP}=0.95$ has a semi-circle plot in the Nyquist diagram indicating the smallest low frequency capacitance value. In comparison, the capacitance of the copolymers with PEDOT, ($X_{PSP}= 0.95$) is higher than the capacitance of PEDOT as a homopolymer ($C_{LF-PEDOT}$: 276.5 mF cm^{-2}).

Table 3.2: ΔQ , thickness of copolymer coated SCFME, C_{LF} and phase angle values for different molar ratios of Poly(EDOT-co-PSP).

Mole Fraction of PSP (X_E)	0.66	0.86	0.90	0.95
ΔQ (mC)	25.08	22.04	11.16	26.70
Thickness of copolymer coated SCFME (μm)	34.5	24.0	21.1	25.46
C_{LF} (mF.cm^{-2})	594.2	1026.3	772.3	408.5
Phase of Z (degree)	71.4°	80.3°	78.5°	58.0°

Figure 3.12 and 3.13 show the Bode magnitude and phase angle plots at which the frequency dependence of the system is more informative compared to the Nyquist plots. The complex plane impedance plots demonstrate a vertical line with phase

angle between 58° - 80° (at 0.01 Hz) and the Bode phase plots also show a peak at around 1000 Hz for $X_{\text{PSP}} = 0.95$. C_{LF} values increase while film resistance values decrease by the increasing of X_{PSP} (Figure 3.14). However all C_{LF} values of copolymers, higher than C_{LF} value of PEDOT.

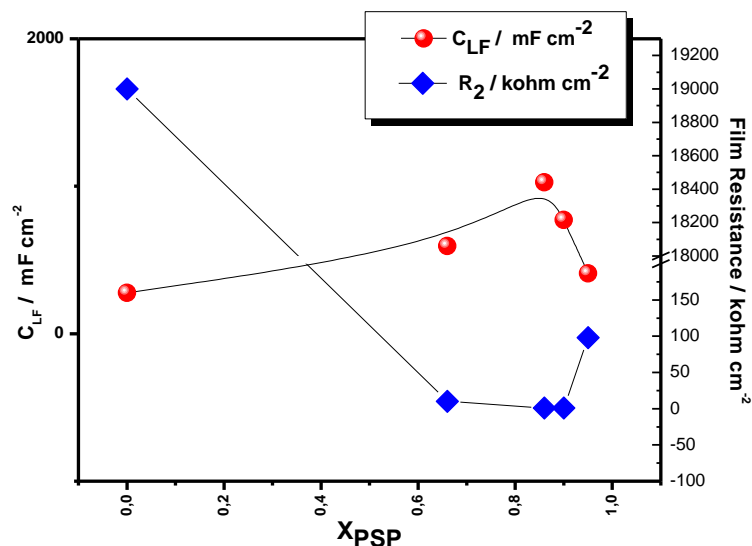


Figure 3.14: Low frequency capacitances (obtained from EIS) and film resistances (obtained from ECM) for different mole fractions of Poly(EDOT-co-PSP) and PEDOT

The electrochemical parameters of the copolymer film in the electrolyte system (NaClO_4 in ACN) were evaluated by using the ZsimpWin (version 3.10) software from Princeton Applied Research. We observed a good agreement between experimental results, the parameters obtained from the best fitting electrical equivalent circuit model, and the chi-squared (χ^2) values minimized. χ^2 is the function defined as the sum of the squares of the residuals.

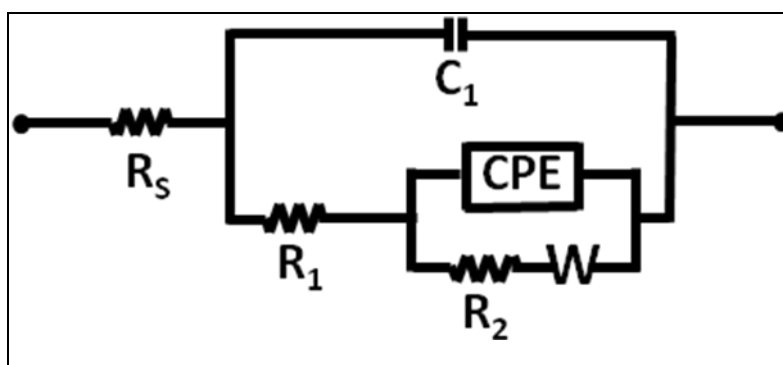


Figure 3.15: Scheme of the equivalent circuit model

An electrical equivalent circuit was used in the simulation of the impedance behavior of the film from the experimentally obtained impedance data. The proposed model (Fig. 3.15) was built using components in series; The first component was the solution resistance of the polymer electrode and the electrolyte, R_s . The second one was the parallel combination of the double layer capacitance, C_{dl} , and the charge transfer resistance in between the polymer electrode and the electrolyte interface, R_1 . The series connection to R_1 was made up using CPE in parallel to R_2 and W , where R_2 is the resistance of the polymer film (with pore-like morphology), and W is the Warburg impedance of diffusion of the ions in the electrolyte.

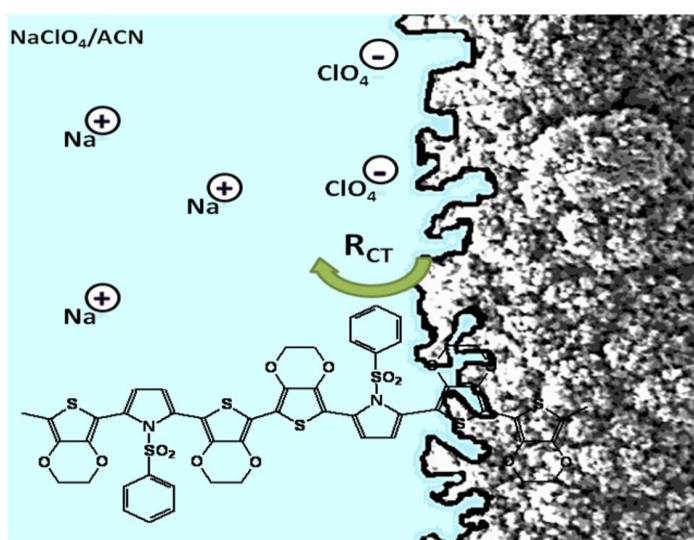


Figure 3.16: Scheme of the interface between copolymer film coated electrode and supporting electrolyte solution (blue part shows the electrolyte, solid part shows the polymer film)

Solvent resistance (R_s) is defined as the sum of resistances due to the electrolyte on the surface or in the pores of the film and 0.1 M NaClO₄/ACN solution. Solvent resistances of copolymers are lower than the solvent resistance of PEDOT as a homopolymer due to the different size of pores of PEDOT and the copolymer; PEDOT has smaller size of pores (Fig. 3.17).

Charge transfer resistance (R_1) shows an increasing trend with PSP inclusion into the copolymer, due to partial destruction of conjugation. Double-layer capacitance (C_1) has also shown a similar behavior. Both of these parameters have exhibited almost linear relationship with the thickness of the film. The film resistance (R_2) was found to be between 0.88 - 10 k Ω cm². The variation of the film resistance could be related to the film thickness as well as the pore distribution and sizes. However, all copolymer films have almost 1000 times lower resistance than the PEDOT film (1.9x10⁴ k Ω cm²).

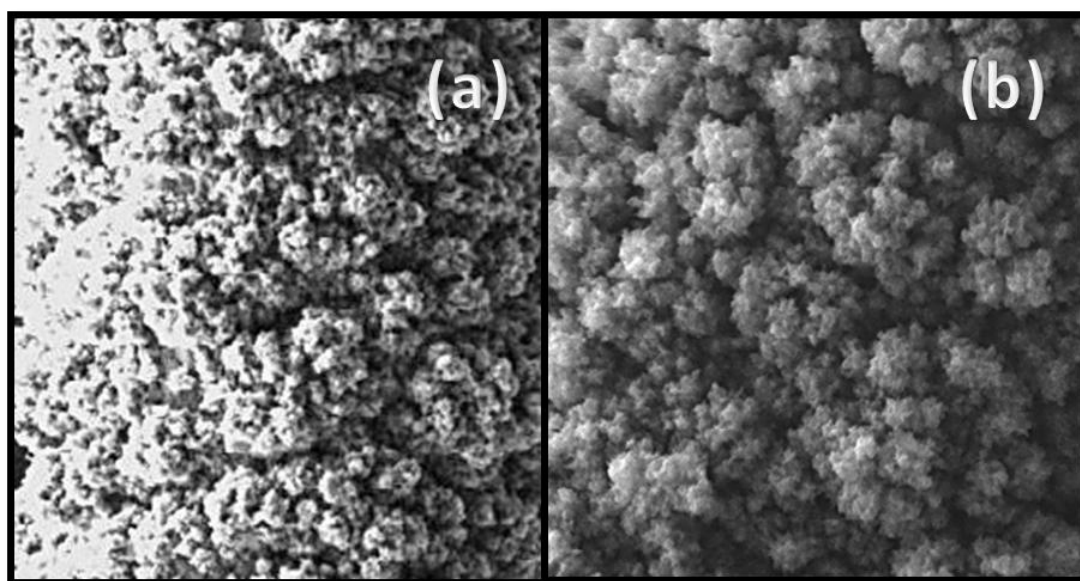


Figure 3.17: SEM images of (a) Poly (EDOT-co-PSP) (scale 20x20 μ m) and (b) PEDOT (scale 30x30 μ m) which show the difference pore formation

CPE was used for fitting the data in to the equivalent circuit, adapting to relatively the non-ideal behavior. The presence of the CPE can be attributed to the electrode roughness or to the inhomogeneity in the conductance or the dielectric constant [91]. n value of CPE is regarded as a major of the inhomogeneity of the copolymer film ($0.72 < n < 1$). If $n=1$, the value of an ideal capacitance can be determined from the

Bode plot. From the definition, $Z_{CPE} = [Q(j\omega)^n]^{-1}$, the parameter Q characterizes properties related to the surface and the electroactive species, ω is the angular frequency ($\omega = 2\pi f$). The exponent n arises from the slope of the $\log Z$ versus $\log f$ plot. In general, the slope of $\log Z$ versus $\log f$ plot (denoted as n) is a manifestation of the electrode nature [92]. n values denote the porosity of the electrode which almost remains constant for $X_{PSP} = 0.00; 0.66; 0.86$. By increasing the PSP amount in copolymer, n values deviate from 1, so Warburg diffusion capacitance prominences. According to the calculations from the equivalent circuit modelling, inclusion of PSP in the copolymer improved capacitance and diffusion properties.

Table 3.3: Mole fraction dependence of parameters calculated from the equivalent circuit model for PEDOT and Poly(EDOT-co-PSP)

$X_{PSP} \rightarrow$	0.00	0.66	0.86	0.90	0.95
$R_s (\Omega\text{cm}^2)$	16.89	7.67	6.05	3.24	7.01
$C_1 (\mu\text{F cm}^{-2})$	2×10^{-5}	0.056	0.052	0.072	0.109
$R_1 (\Omega\text{cm}^2)$	2.56	3.36	5.30	3.57	7.83
$CPE; Y_o (\text{S s}^{-n} \text{cm}^{-2})$	0.016	5.135	0.566	0.102	0.156
n	0.97	0.99	1.00	0.72	0.86
$R_2 (\text{k}\Omega\text{cm}^2)$	1.9×10^4	10.00	0.87	1.00	0.98
$W; Y_o (\mu\text{S s}^{-0.5} \text{cm}^{-2})$	5.0×10^{-14}	3.3×10^{-7}	230	1180	8000
χ^2	2.0×10^{-3}	4.2×10^{-4}	5.2×10^{-3}	9.6×10^{-4}	5.0×10^{-3}

3.6 Morphological Analyses of Poly(EDOT-co-PSP) Films via SEM and AFM

Morphological analysis were made via SEM and AFM. SEM images of Poly(EDOT-co-PSP) copolymers, obtained at 5 kV, were examined, and illustrated in Fig. 3.17. PEDOT film has nanostructure (pores) depending on the preparation conditions. Copolymer morphology is very similar for all mole fractions and Poly(EDOT-co-PSP) copolymers have larger pores when compared to PEDOT (Fig. 3.18). For the case examined, Poly(EDOT-co-PSP) appears to hold a cauliflower shape, with large sizes of pores.

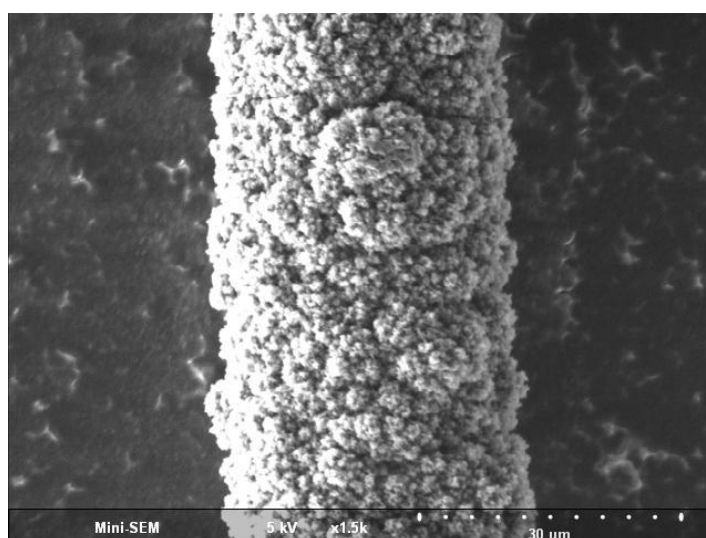


Figure 3.18: SEM image of the copolymer coated SCFME with a mole fraction of PSP of 0.66

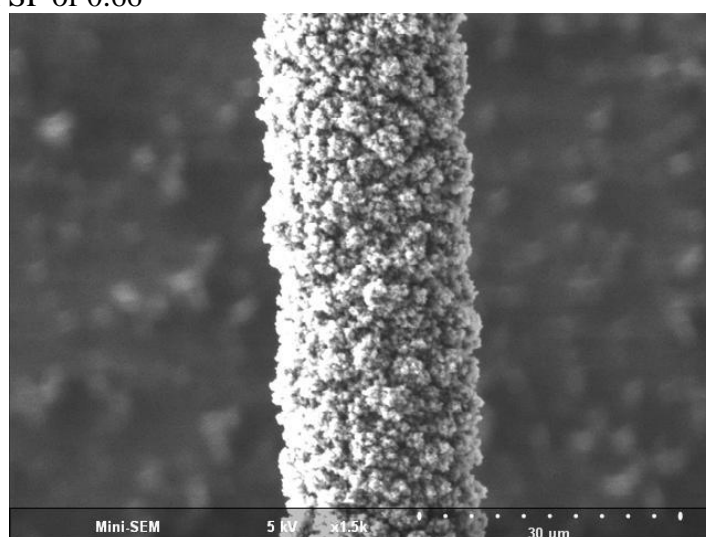


Figure 3.19: SEM image of the copolymer coated SCFME with a mole fraction of PSP of 0.86

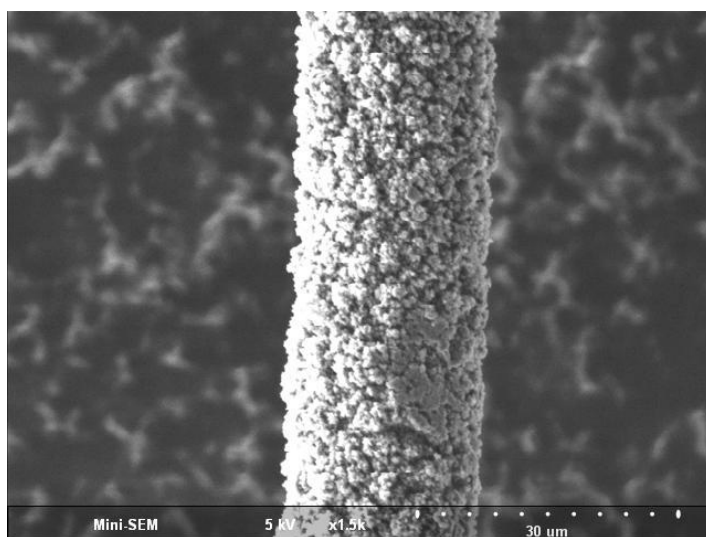


Figure 3.20: SEM image of the copolymer coated SCFME with a mole fraction of PSP of 0.90

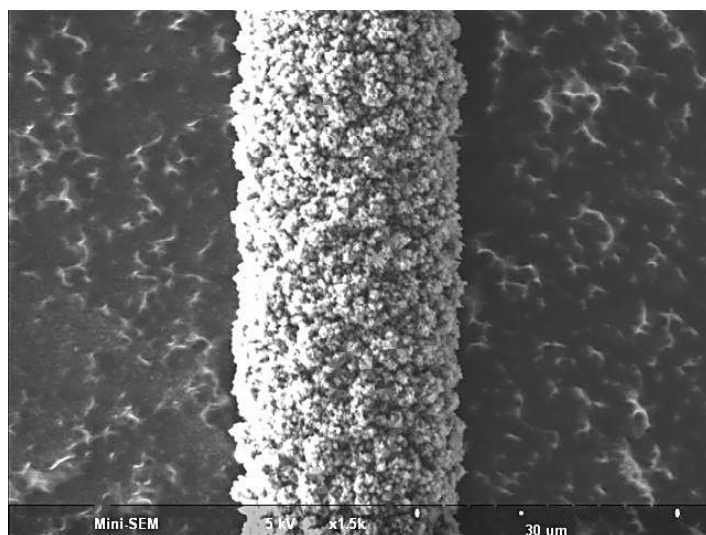


Figure 3.21: SEM image of the copolymer coated SCFME with a mole fraction of PSP of 0.95

For AFM analyses of poly(EDOT-co-PSP) synthesized onto Boron-doped p-type silicon wafer (0.001 ohm/cm). Chronoamperometry method was performed by using 1.66 mM EDOT and 10 mM PSP ($X_{\text{PSP}} = 0.86$) at 0.8V in 0.1 M NaClO₄/ACN electrolyte solution. A Blue-black homogenous film was obtained on the silicon wafer and washed with ACN to remove the unpolymerized monomers. The roughness analyses were performed on a smaller area on the silicon wafer. Poly(EDOT-co-PSP) coated surface has 51.44 nm roughness (for 7.62 μm^2 area)

with a cauliflower-like structure, which have been reported for poly[1-(4-Methoxyphenyl)-1H-Pyrrole] in [93] (Fig. 3.22).

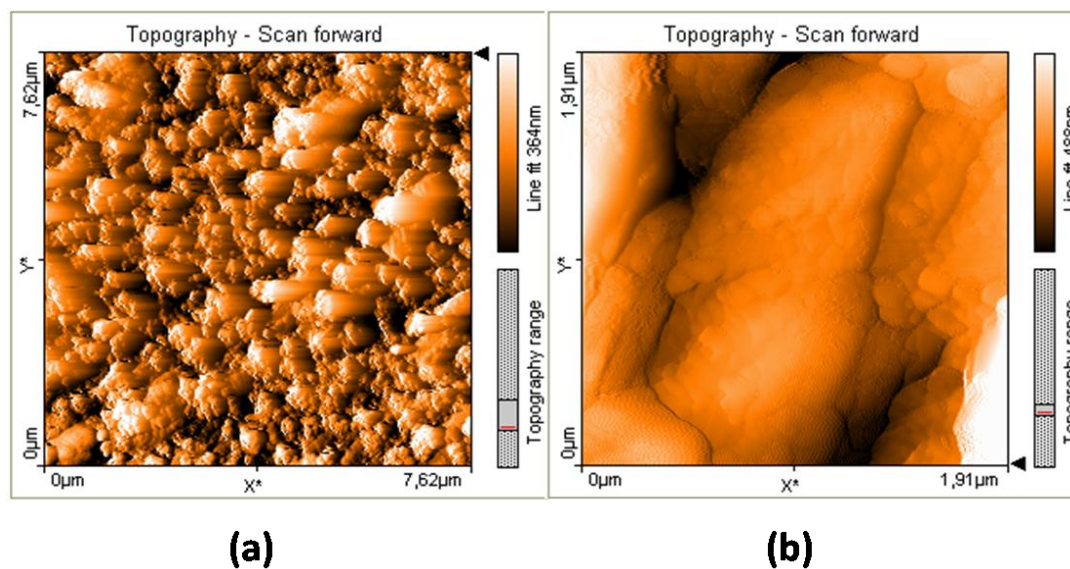


Figure 3.22: AFM topographies of Poly(EDOT-co-PSP) coated silicon wafer at (a) 7.62 μm x 7.62 μm and (b) 1.91 μm x 1.91 μm

4. CONCLUSIONS

3,4-(Ethylenedioxythiophene) and N-phenylsulfonyl pyrrole was electrochemically copolymerized on single carbon fiber micro electrodes in different mole fractions of N-phenylsulfonyl pyrrole and then morphologic, spectroscopic and the electrochemical characterizations of the films were studied.

Deposition conditions on the carbon fiber and the influence of the monomer concentrations on the resulting copolymer have shown higher capacitance can be synthesized for $X_{\text{PSP}}=0.86$. EIS and ECM were employed to characterize the electrochemical behaviour of electrochemically prepared Poly(EDOT-co-PSP) films in $\text{NaClO}_4/\text{ACN}$.

FTIR-ATR characteristic peaks of PSP indicates the inclusion into copolymer. The changing of the capacitance of the copolymer is reflected on to the equivalent circuit model by the dependency of the mole fractions. Inclusion of PSP in the copolymer improved capacitance and diffusion properties proved by equivalent circuit modelling.

REFERENCES

- [1] **Nalwa, H.S.**, 1997. *Handbook of Organic Conductive Molecules and Polymers*, vol.1-4, Wiley, Chichester, UK.
- [2] **Skotheim, T.A., Elsenbaumer, R.L. and Reynolds, J.R.**, 1998. *Handbook of Conducting Polymers*, 2nded., Marcel Dekker, New York.
- [3] **Storsberg, J., Ritter, H., Pielartzik, H. and Groenendaal, L.**, 2000, Cyclodextrins in polymer synthesis: Supramolecular cyclodextrin complexes of pyrrole and 3-ethylenedioxythiophene and their oxidative polymerization, *Adv.Mater.*, **12(8)**, 567-569.
- [4] **Inzelt, G., Pineri, M., Shultze, J.W. and Vorotyntsev, M.A.** 2000, Electron and proton conducting polymers: Recent development and prospects, *Electrochim.Acta*, **45(15-16)**, 2403-2421.
- [5] **Heeger, A.J.** 2001, Semiconducting and metallic polymers: The fourth generation of polymeric materials, *J.Phys.Chem.B.*, **105(36)**, 8475-8491.
- [6] **Diaz, A.F., Kanazawa, K.K. and Gardini, G.P.**, 1979, Electrochemical Polymerization of pyrrole, *J.Chem.Soc.Chem.Comm.*, **14**, 635-636.
- [7] **Hepburn, A.R., Marshall, and Maud J.M.**, 1991, Novel electrochromic films via anodic-oxidation of carbazolyl substituted polysiloxanes, *Synth.Met.*, **43(1-2)**, 2935-2938.
- [8] **Mastragostino, M., Marinangeli, A.M., Corradini, A. and Giarcobbe, S.**, 1989, Conducting polymers as electrochromic materials, *Synth.Met.*, **28(1-2)**, C501-C506.
- [9] **Dubios, J.C. Sagnes O. and Henry F.**, 1989, Polyheterocyclic conducting polymers and composites derivatives, *Synth.Met.*, **28(1-2)**, C871-C878.
- [10] **Roncali, J., Garrerau, R., Delabouglise, D., Garnier, F. and Lemaire, M.**, 1989, Modification of the structure and electrochemical properties of poly(thiophene) by ether groups, *J.Electroanal.Chem.*, **269(2)**, 337-349.
- [11] **Saleneck, W.R.**, Science and applications of conducting polymers, proc of the 6th Europhysics Industrial workshop, Adam Hilger (1991).
- [12] **Bradley, D.D.C.**, 1991, Molecular electronics-aspects of the physics, Chemistry in Britain, **27(8)**, 719-723.
- [13] **Roncali, J.** 1999, Electro-generated functional conjugated polymers as adv. electrode materials, *J.Mater.Chem.*, **9(9)**, 1875-1893.
- [14] **Reddinger, J.L. and Reynolds, J.R.**, 1999, Molecular engineering of π -conjugated polymers, *Adv. Polym.Sci.*, **145**, 57-122.

- [15] **Heinze, J.**, Topics in Current Chemistry, *Springer-Verlag*, Berlin, 152 (1990) 2.
- [16] **Gerard, M., Chaubey A. and Mallhotra, B. D.**, 2002, Application of conducting polymers to biosensors, *Biosensors and Bioelectronics*, **17(5)**, 345-359.
- [17] **Doblhofer, K. and Rajeshwar, K.**, Handbook of Conducting Polymers (1998), 531.
- [18] **Kawde, R.B. and Santhanam, K.S.V.**, 1995, An in-vitro electrochemical sensing of dopamine in the presence of ascorbic acid, *Bio-electrochemistry and Bio-energetics*, **38(2)**, 405-409.
- [19] **Kawde, R.B., Laxmeshwar, N.B. and Santhanam, K.S.V.**, 1994, Cyclic voltammetric oxidation of L-dopant at polycarbazole-modified electrode evaluation of the cyclization rate-constant, *Bioelectrochem. Bioenergetics*, **34(1)**, 83-85.
- [20] **Wu, Z.Y., Jing, W.G. and Wang, E.**, 1999, Oxidation of NADH by dopamine incorporated in lipid film cast onto a glassy carbon electrode, *Electrochem. Commun.*, **1(11)**, 545-549.
- [21] **Kumru, M.E., Springer, J., Sarac, A.S. and Bismarck, A.**, 2001, Electrografting of thiophene, carbazole, pyrrole and their copolymers onto carbon fibers, electro-kinetic measurements, surface composition and morphology, *Synth. Met.*, **123(3)**, 391-402.
- [22] **Sarac, A.S., Bismarck, A., Kumru, M.E. and Springer, J.**, 2001, Electrografting of poly(carbazole-co-acrylamide) onto several carbon fibers-Electro-kinetic and surface properties, *Synth. Met.*, **123(3)**, 411-423.
- [23] **Bismarck, A., Menner, A., Kumru, M.E., Sarac, A.S., Bistriz, M. and Shulz, E.**, 2002, Poly(carbazole-co-acrylamide) electrocoated carbon fibers and their adhesion behavior to an epoxy resin matrix, *J.Mater.Sci.*, **37(3)**, 461-471.
- [24] **Sarac, A.S. and Springer, J.**, 2002, Electrografting of 3-methyl thiophene onto carbon fiber: Characterization and carbazole random copolymer by FTIR-ATR, SEM, EDX, *Surf. & Coat. Technol.*, **160(2-3)**, 227-238.
- [25] **Miller, J.S.**, 1993, Conducting polymers-materials of commerce, *Adv.Mater.*, **5(7-8)**, 587-589.
- [26] **Miller, J.S.**, 1993, Molecular materials 7.B. conducting polymers-materials of commerce, *Adv. Mater.*, **5(9)**, 671-676.
- [27] **Thompson, B.C., Schottland, P., Zong, K.W. and Reynolds, J.R.**, 2000, In situ colorimetric analysis of electrochromic polymers and devices, *Chem.Mater.*, **12(6)**, 1563-1571.
- [28] **Burn, P.L., Holmes, A.B., Kraft, A., Bradley, D.D.C., Brown, A.R., Friend, R.H. and Gymer, R.W.**, 1992, Chemical tuning of electroluminescent copolymers to improve emission efficiencies and allow patterning, *Nature*, **356(6364)**, 47-49.

- [29] **Gazotti, W.A., Casalbore-Miceli, G., Geri, A., Berlin, A. and De Paoli, M.A.,** 1998, An all-plastic and flexible electrochromic device based on elastomeric blends, *Adv. Mater.*, **10(18)**, 1522-1525.
- [30] **Inganas, O., Johanson T. And Ghosh, S.,** 2001, Phase engineering for enhanced electrochromism in conjugated polymers, *Electrochim. Acta.*, **46(13-14)**, 2031-2034.
- [31] **Sotzing, G.A., Reynolds, J.R. and Steel, P.J.,** 1997, Poly(3,4-ethylenedioxythiophene) (PEDOT) prepared via electrochemical polymerization of EDOT, 2,2'-bis (3,4-ethylenedioxythiophene) (BEDOT), and their TMS derivatives, *Adv.Mater.*, **9(10)**, 795-798.
- [32] **Sapp, S.A., Sotzing and G.A., Reynolds, J.R.,** 1998, High contrast ratio and fast-switching dual polymer electronic devices, *Chem.Mater.*, **10(8)**, 2102-2108.
- [33] **Sapp, S.A. Sotzing, G.A., Reddinger, J.L. and Reynolds, J.R.,** 1996, Rapid switching solid state electronic devices based on complementary conducting polymer films, *Adv.Mater.*, **8(10)**, 808-811.
- [34] **Rauh, R.D., Wang, F., Reynolds, J.R. and Meeker, D.L.,** 2001, High coloration efficiency electrochromics and their application to multicolor devices, *Electrochim.Acta*, **46(13-14)**, 2023-2029.
- [35] **Bard, A.J. and Faulkner, L.R.,** 2001, Electrochemical methods: fundamentals and applications, John Wiley, New York.
- [36] **Lyons, M.E.G.,** 1997, Advances in Chemical Physics, *Polymeric Systems*, John Wiley&Sons New York.
- [37]
- [38] **Jenden, C.M., Davidson, R.G. and Turner, T.G.,** 1993, A fourier transform-raman spectroscopic study of electrically conducting polypyrrole films, *Polymer*, **34(8)**, 1649-1652.
- [39] **Waltman, R.J. and Bargon, J.,** 1985, The electropolymerization of polycyclic hydrocarbons-substituent effects and reactivity structure correlations, *J. Electroanal. Chem.*, **194(1)**, 49-62.
- [40] **Bauerle, P., Segelbacher, U., Maier, A. and Mehring, M.,** 1993, Electronic structure of monomeric and dimeric cation radicals end-capped oligothiophenes, *J.Am.Chem.Soc.*, **115(22)**, 10217-10223.
- [41] **Kassim, A., Davis, F.J. and Mitchell, G.R.,** 1994, The role of the counter-ion during electropolymerization of polypyrrole camphor sulfonate films, *Synth.Met.*, **62(1)**, 41-47.
- [42] **Warren, L.F. and Anderson, D.P.,** 1987, Polypyrrole films from aqueous electrolytes-the effect of anions upon order, *J. Electrochem Soc.*, **134(1)**, 101-105.
- [43] **Li, Y.F. and Yang, J.,** 1997, Effect of the electrolyte concentration on the properties of the electropolymerized polypyrrole films, *J.Appl.Poly.Sci.*, **65(13)**, 2739-2744.

- [44] **Bauerle, P. And Scheib, S.**, 1993, Molecular recognition of alkali ions by crown-ether functionalized poly(alkylthiophenes), *Adv. Mater.*, **5(11)**, 848-853.
- [45] **Imanishi, K., Satoh, M., Yasuda, Y., Tsushima, R. and Aoki, S.**, 1988, Solvent effect on electrochemical polymerization of aromatic compounds, *J.Electroanal.Chem.*, **242(1-2)**, 203-208.
- [46] **Diaz, A.F. and Bargon, I.**, 1986. "Handbook of Conducting Polymers", 1st ed., Ed.T.J. Skotheim, Marcel Dekker, New York, 1337.
- [47] **Funt, R.L. and Diaz, A.F.**, 1991, "Organic Electrochemistry: an Introduction and a Guide", Marcel Dekker, New York, 1337.
- [48] **Ko, J.M., Rhee, H.W., Park, S.M. and Kim, C.Y.**, 1990, Morphology and electrochemical properties of polypyrrole films prepared in aqueous solvents, *J.Electrochem.Soc.*, **137(3)**, 905-909.
- [49] **Unsworth, J., Innis, P.C., Lunn, B.A., Jin, Z. and Norton, G.P.**, 1992, The influence of electrolyte pH on the surface-morphology of polypyrrole, *Synth.Met.*, **53(1)**, 59-69.
- [50] **Jones, D., Guerra, M., Favaretto, L., Modelli, A. and Fabrizio, M.**, 1990, Determination of the electronic structure of thiophene oligomers and extrapolation of polythiophene, *J.Phys.Chem.*, **94(15)**, 5761-5766.
- [51] **Suarez, M.F. and Campton, R.G.**, 1999, In-situ atomic force microscopy study of polypyrrole synthesis and the volume changes induced by oxidation and reduction of the polymer, *J.Electroanal.Chem.*, **462(2)**, 211-221.
- [52] **Rodriguez, J., Grande, H.J. and Otero, T.F.**, 1997, Handbook of Organic Conducting Molecules and Polymers, John Wiley & Sons, 415.
- [53] **Chandrasekhar, P., Zay, B.J., Ross, D., McQueeney, T., Birur, G.C., Swanson, T., Kauder, L. and Douglas, D.**, 2002, Conducting polymer based dynamic IR-electrochromics for spacecraft thermal control, Abst. Papers Am. Chem.Soc., **223 D25 287-Poly Part-2**.
- [54] **Roncali, J.**, 1992, Conjugated poly(thiophenes)-synthesis, functionalization and applications, *Chem.Rev.*, **92(4)**, 711-738.
- [55] **Groenendal, L.B., Jonas, F., Freitag, D., Pielartzik, H., Reynolds, J.R.**, 12 (2000) 481.
- [56] **Tourillon, G., Garnier, F.**, 1984, *J.Electroanal.Chem.* Interfacial Electrochem., 161, 51.
- [57] **Jonas, F., Schrader, L.**, 1991, *Synth.Met.*, 41-43, 831.
- [58] **Czardybon, A., Lapkowski, M.**, 2001, Synthesis and electropolymerisation of 3,4-ethylenedioxythiophene functionalised with alkoxy groups, *Synth. Met.*, **119(1-3)**, 161-162.
- [59] **Carlberg, J.C., Inganas, O.**, 1997, Poly(3,4-ethylenedioxythiophene) as electrode material in electrochemical capacitors., *J.Electrochem. Soc.*, **144(4)**, L61.

- [60] **Jonas, F., Morrison, J.T.**, 1997, 3,4-Polyethylenedioxythiophene (PEDT): Conductive coatings technical applications and properties, *Synth. Met.*, **85(1-3)**, 1397-1398.
- [61] **Pei, Q.B., Zuccarello, G., Ahlskog, M., Inganas, O., Inganas**, 1994, Electrochromic and highly stable poly(3,4-ethylenedioxythiophene) switches between opaque blue-black as transparent sky blue, *Polymer*, **35(7)**, 1347-1351.
- [62] **Sotzing, G.A., Reddinger, J.L., Reynolds, J.R., Steel, P.J.**, 1997, Redox active electrochromic polymers from low oxidation monomers containing 3,4-ethylenedioxythiophene (EDOT), *Synth. Met.*, **84(1-3)**, 199-201.
- [63] **Carlberg, C., Chen, X.W., Inganas, O.**, 1996, Ionic transport and electronic structure in poly(3,4-ethylenedioxythiophene), *Solid State Ionics*, **85(1-4)**, 73-78.
- [64] **Gusstafson, J.C., Liedberg, B., Inganas, O.**, 1994, In situ spectroscopic investigations of electrochromism and ion transport in a poly(3,4-ethylenedioxythiophene) electrode in a solid state electrochemical cell, *Solid State Ionics*, **69(2)**, 145-152.
- [65] **Yamato, H., Ohwa, M., Wernet, W.**, 1995, Stability of polypyrrole and poly(3,4-ethylenedioxythiophene) for biosensor application, *J. Electroanal. Chem.*, **397(1-2)**, 163-170.
- [66] **Lee, Y., Park, S., Lee, J.**, 1999, Synthesis and characterization of a soluble conducting polymer, poly(3,4-ethylenedioxythiophene), *Polymer (Korea)*, **23(1)**, 122-128.
- [67] **Randriamahazaka, H., Noel, V., Chevrot, C.**, 1999, Nucleation and growth of poly(3,4-ethylenedioxythiophene) in acetonitrile on platinum under potentiostatic conditions, *J. Electroanal. Chem.*, **472(2)**, 103-111.
- [68] **Sakmeche, N., Aeiyaeh, S., Aaron, J.J., Jouini, M., Lacroix, J.C., Lacaze, P.C.**, 1999, Improvement of the electrosynthesis and physicochemical properties of poly(3,4-ethylenedioxythiophene) using a sodium dodecyl sulfate micellar aqueous medium, *Langmuir*, **15(7)**, 2566-2574.
- [69] **Sarac, A.S., Gilsing, H.D., Gencturk, A., Schulz, B.**, 2007, Electrochemically polymerized 2,2-dimethyl-3,4-ethylenedioxythiophene on carbon fiber for microsupercapacitor, *Prog. Org. Coat.*, **60(4)**, 281-286.
- [70] **Yurtsever, M., Sonmez, G., Sarac, A.S.**, 2003, Time dependent density functional theory calculations for the electronic excitations of pyrrole-acrylamide copolymers, *Synth. Met.*, **135-136**, 463-464.
- [71] **Sarac, A.S., Sonmez, G., Cebeci, F.C.**, 2003, Electrochemical synthesis and structural studies of polypyrroles, poly(3,4-ethylenedioxythiophene)s and copolymers of pyrrole and 3,4-ethylenedioxythiophene on carbon fiber micro electrode, *Appl. Electrochem.*, **33(3-4)**, 295-301.

- [72] **Oliver, R., Munoz, A., Ocampo, C., Aleman, C., Armelin, E., Estrony, F.,** 2006, Electrochemical characteristics of copolymers electrochemically synthesized from N-methyl pyrrole and 3,4-ethylenedioxythiophene on steel electrodes: comparison with homopolymers, *Chem. Physic.*, **328(1-3)**, 299-306.
- [73] **Chang, C.C., Her, L.J., Hong, J.L.,** 2005, copolymerization from electropolymerization of thiophene and 3,4-ethylenedioxythiophene and its use as cathode for lithium ion battery, *Electrochim. Acta*, **50(22)**, 4461-4468.
- [74] **Alpatova, N.M., Ovsyannikova, E.V., Jonas, F., Kirmeyer, S., Pisarevskoya, E.Y., Grosheva, M.Y.,** 2002, Redox conversions poly(3,4-ethylenedioxythiophene) and its copolymer with bithiophene in aprotic media of different donor capability, *J.Electrochem.*, **38(6)**, 576-582.
- [75] **Yohannes, T., Carlberg, J.C., Inganas, O., Solomon, T.,** 1997, electrochemical and spectroscopic characteristics of copolymers electrochemically synthesized from 3-methylthiophene and 3,4-ethylenedioxythiophene, *Synth.Met.*, **88**, 15-21.
- [76] **Geißler, U., Hallensleben, M.L., Toppare, L.,** 1993, Electrochemical studies on carbazole/pyrrole copolymers, *Synth.Met.*, **55(2-3)**, 1483-1488.
- [77] **Xu, J., Nie, G., Zhang, S., Han, X., Hou, J., Pu, S.,** 2005, Electrochemical copolymerization of indole and 3,4-ethylenedioxythiophene, *J.Mater.Sci.*, **40(11)**, 2867-2873.
- [78] **Castello B.P.J.L., Evans, P., Guernion, N., Ratcliffe, N.M., Sivanand, P.S., Teare, G.G.,** 2000, The synthesis of a number of 3-alkyl and 3-carboxy substituted pyrroles: their chemical polymerisation onto poly(vinylidene fluoride) membranes and their use as gas sensitive resistor, *Synth.Met.*, **114(2)**, 181-188.
- [79] **Janosik, T., Shirani, H., Whalstorm, N., Malky, I., Stensland, J., Bergman, J.,** 2006, Efficient sulfonation of 1-phenylsulfonyl-1-H-pyrroles and 1-phenylsulfonyl-1-H-indoles using chronosulfonic acid in acetonitrile, *Tetrahedron*, **62(8)**, 1699-1707.
- [80] **Parsons, R.,** 1990, Electrical double layer recent experimental and theoretical developments, *Chemical Reviews*, **90**, 813-826.
- [81] **Randles, J.E.B.,** 1948, A cathode ray polarograph: Part II the current voltage curves, *Transactions of the Faraday Society*, **44**, 327-338.
- [82] **Buck, R.P., Mundt, C.,** 1999, *Electrochim. Acta*, **44**, 1999.
- [83] **Macdonald, J.R.,** 1990, *Electrochim. Acta*, **35**, 1483.
- [84] **Ding, H., Pan, Z., Pigani, L., Seeber, R.,** 2001, *J.New.Mater.Electrochem.Sys.*, **4**, 63.
- [85] **Duffitt, G.L., Pickup, P.G.,** 1991, *J.Phys.Chem.*, **95**, 964.
- [86] **Duffitt, G.L., Pickup, P.G.,** 1992, *J.Chem.Soc., Faraday Trans.*, **88**, 1417.
- [87] **Albery, W.J., Mount, A.R.,** 1994, in: M.E.G. Lyons (Ed.), *Electrocative Polymer Electrochemistry*, vol I, Plenum Press, New York.

- [88] **Jackson, M.L.**, 1985, *Soil Chemical Analysis*, Ed.2, 650-14.
- [89] **Glasstone**, 1946, *Textbook of Physical Chemistry*, Ed.2, pp947-9.
- [90] **Sezer, E., Ustamehmetoglu, B., Sarac, A.S.**, 1999, Chemical and Electrochemical polymerization of pyrrole in the presence of N-substituted carbazole, *Synth.Met.*, **107(1)**, 7-17.
- [91] **Göhr, H., Bunsenges. B.**, 1981, *Phys. Chem*, 85, 274.
- [92] **Girija, T.C., Sangaranarayanan, M.V.**, 2006, Investigation of polyaniline-coated stainless steel electrodes for electrochemical supercapacitors, *Synth. Met.*, **156(2-4)**, 244-250.
- [93] **Sarac, A.S., Sezgin, S., Ates, M., Turhan, C.M.**, 2009, Electrochemical Impedance Spectroscopy and morphological analyses of pyrrole, phenylpyrrole and methoxyphenylpyrrole on carbon fiber micro electrodes, *Surface and Coat. Tech.*, **202(16)**, 3997-4005.

CURRICULUM VITAE



Candidate's full name	: Cansev TEZCAN
Place and date of birth	: Arhavi - 01/01/1987
Permanent address	: İhlamur / Beşiktaş
Universities attended	: İstanbul Technical University – İSTANBUL Polymer Science and Technology – 09/2008 – 06/2010 Eskişehir Osmangazi University – ESKİŞEHİR Chemistry – 09/2004 – 07/2008